FLAT-SLAB STRENGHTENING TECHNIQUES AGAINST PUNCHING-SHEAR

Massimo Lapi[1], Antonio Pinho Ramos[2], Maurizio Orlando[3]

[1]PhD Candidate, DICEA, Università degli Studi di Firenze, Via di Santa Marta n.3, 50139, Firenze, Italy

[2]Professor, CERIS, ICIST, Faculdade de Ciências e Tecnologia da Universidade NOVA de Lisboa, Departamento de Engenharia Civil. ampr@fct.unl.pt

[3]Associate Professor, DICEA, Università degli Studi di Firenze, Via di Santa Marta n.3, 50139, Firenze, Italy

1. ABSTRACT

Over the years, the flat slab system has become a popular form of construction in many countries, particularly for multi-storey buildings such as offices or carparks. Nowadays, a considerable number of flat slab buildings requires strengthening against punching. Reasons are several, like design or construction errors, poor quality materials, not complying with new codes provisions, or increase of vertical load. This paper discusses different techniques for strengthening of R/C slabs against punching: addition of post-installed shear reinforcement, gluing external fibre reinforced polymers, casting a bonded reinforced concrete overlay (BRCO) on the slab's top surface, enlargement of the support or application of a post-tensioning system. The authors compared the strengthening techniques using the Critical Shear Crack Theory (CSCT) in order to evaluate the effectiveness of each one. This paper shows that the CSCT could be easily adapted to all of these techniques, moreover predicted values of the punching strength are in good agreement with literature experimental results. The aim of this work is to provide designers with the tool to choose which strengthening technique suits better to the specific case.

2. INTRODUCTION

A flat slab is a two-way reinforced concrete structural element, which carries vertical and horizontal load and transfers it directly to columns, without beams or girders. One of the most important issues of a flat-slab is the concentration of shear and bending stresses in the proximity of columns, which may lead to punching failure. Punching is given by a local failure mechanism associated with the formation of a truncated cone shape. It has a brittle nature, as it occurs with limited warning signs, and, in absence of integrity reinforcement, could bring to a progressive collapse of the entire building. Over the years, the flat slab system has become a popular form of construction in many countries, particularly for multi-storey buildings. Nowadays, a considerable number of flat slab buildings requires strengthening against punching [1]. Reasons are several, like design or construction errors, environmental deterioration of materials, not complying with new codes provisions, or at the least increase of vertical load.

The occurrence of design and construction errors, accompanied by environmental deterioration brought in 1997 to the partial collapse by punching of the Piper Row Car Park at Wolverhampton. The car park was built in 1965 adopting a particular technique: the slabs where casted on the ground floor and lifted on precast columns. Slabs were supported on steel wedges fixed to shear collars. As reported by Wood [2] the design of the car park was performed in 1964 ignoring tolerances on support wedges and detailing of the shear collars. The concrete strength was highly variable and in localized areas was lower than the specified strength of 20.5 MPa. The poor quality of concrete increased the susceptibility to deterioration, indeed

since 1987 the car park required substantial repairs. After several inspections, in January 1997 a crack found near a column was considered potentially serious, however before the detailed inspection the structure collapsed completely on 20th March 1997.

In 1995 the Sampoong department store in Seoul collapsed by punching, killing more than 500 persons. Contrary to the previous case there was no environmental deterioration since the building was opened on December 1989. As reported by Gardner et al. [3] several construction deficiencies were identified: concrete strength of 18 MPa rather than the specified value of 21 MPa, effective slab depth in the negative moment areas reduced from the specified 410 to 360 mm, column diameter supporting the collapsed slab was only 600 mm instead of the specified 800 mm. Finally, the use of the collapsed floor was changed increasing the loads by 35%. Despite signals of structural distress were evident in several locations before the collapse of the building, the authorities took no action to avoid such failure.

The most important lesson provided by these episodes is that an adequate inspection and a subsequently strengthening intervention would have avoided such collapses. To meet this new demand for repairing existing buildings, several techniques have been developed. Strengthening techniques against punching of R/C flat-slabs could be grouped into four types: shear strengthening, flexural strengthening, enlargement of the support and post-tensioning systems.

Shear strengthening represents one of the first strengthening technique against punching investigated by the researchers, it is performed through the installation of steel bolts or other shear reinforcements. In 1974 Ghali et al. [4] investigated the insertion of prestressed unbonded steel bolts around the column. In 1996 Hassanzadeh [5] proposed the use of bonded shear reinforcement. Later Ramos et al. [6] studied the insertion of post-installed steel bolts on damaged slabs. In 2003 El-Salakawi et al. [7] proposed the use of post-installed shear bolts (the shear bolt consists of a headed vertical rod threaded at the other end for anchoring using a washer and nut system). Inácio et al. [8] studied different anchorage approaches for post-installed steel bolts, later Askar [9], [10] investigated the effect of steel stud with or without steel plates placed on the top and bottom of the slab. In recent years other types of shear reinforcement have been investigated, they differ from the others for the use of composite materials. Binici and Bayrak proposed the use of carbon fiber reinforced polymers (CFRP) strips as vertical shear reinforcement like stirrups [11], [12], later Meisami et al. investigated CFRP rods, grids and fans [13]–[15]. Recently, Gouveia et al. [16] highlighted that the use of FRC allow for increase ductility of the slab similarly to the application of shear reinforcement.

Flexural strengthening consists in gluing external FRP strips on the top of the slab, Karbahari et al. [17] represents one of the first investigation about this technique on R/C slabs. Ayman and Khalid Mosallam [18] tested this strengthening technique on both reinforced and unreinforced concrete slabs. In 2004 Ebead and Marzok [19] evaluated the differences between Carbon FRP strips (CFRP) and Glass FRP laminates (GFRP). Chen and Li [20] highlighted an increase of flexural capacity thanks to the FRP strengthening but also a decrease in ductility. Kim et al. [21] and Abdullah et al. [22] showed the difference between non-prestressed and prestressed FRP plates. Esfahani et al. [23] showed the behaviour of strengthened slabs with CRP under cyclic vertical loading. Finally, Faria et al. [24] proposed a new method to predict the punching capacity of strengthened slabs with FRP, based on the Critical Shear Crack Theory (CSCT), the mechanical model developed by Muttoni in 2008 [25].

The enlargement of the support may be obtained through the insertion of concrete or steel capital or widening the column section. In 1996 Hassanzadeh [5] investigated the insertion of both concrete and steel

capitals. The experimental results showed that the new capital worked as a column built with a column head from the beginning [26]. In 2000 Ramos et al. [6] studied the effect of post-installed steel beams acting as a column head. Later Widianto [27] investigated the rehabilitation of damaged slabs through the insertion of steel collars clamped to the column under the slab.

Concerning the last strengthening technique, which uses post-tensioning systems, recently, various types of prestressing systems have been adopted for the rehabilitation of existing slabs. Such techniques could be grouped to categories: shear strengthening and flexural strengthening. Faria et al. [28], [29] investigated shear strengthening by introducing post-tensioned steel strands anchored through bonding. Later Keller et al. [30], [31] studied the application of prestressed CFRP straps with different types of anchorage. The influence of post-tensioning is found not only on deviation forces and in-plane forces of the tendons but also on bending moment due to tendon eccentricities [32]. Flexural prestressing systems consist in installing and prestressing FRP strips on the tension face of the slab. The first application of this technique on two-way slabs is due to Longworth et al. [33] in 2004, later Kim et al. [21] focused mainly on the flexural behaviour of the strengthened slab. Finally, Abdullah et al. [22] highlighted that using prestressed FRP plates does not enhance the ultimate behaviour as much as non-prestressed FRP plates.

Finally, the application of bonded reinforced concrete overlay (BRCO) on the slab's top, allows for both flexural and punching-shear strengthening. The investigations about this technique applied to reinforced concrete flat slabs are essentially due to Fernandes et al. [34], [35]. Recently, Lapi et al. [36] developed and ad hoc method, grounded on the Critical Shear Crack Theory (CSCT) [25], for the prediction of the punching capacity of slabs strengthened using BRCO.

In this paper the main strengthening techniques against punching shear are presented and discussed. For each technique the CSCT is applied to determine the punching capacity after strengthening. Some applications of the CSCT, specifically thought for strengthening, are already available in literature and are reported here, while others are developed by the authors. In particular Ruiz et al. [37] applied the CSCT to slabs strengthened with bonded post-installed steel shear reinforcement. In this paper the application proposed by Ruiz et al. [37] is extended to other types of shear reinforcements like unbonded bolts and FRP fans or grids. The applications of the CSCT to slabs strengthened with FRP strips and BRCO are provided by Faria et al. [24] and Lapi et al. [36], respectively. The application of the CSCT to slab strengthened through enlargement of the support is provided by the authors and it is discussed in the following. With regards to post-tensioning systems, the application of the CSCT is derived by the authors starting from previous works [32], [38] focused on post-tensioned slabs. The predictive capability of the CSCT, with the additional applications, is evaluated by comparing the theoretical punching strength with experimental results available in literature.

3. STRENGTHENING TECHNIQUES

3.1 Mechanical approach for the determination of the punching strength

Following the theory developed by Muttoni [25] the punching strength is found at the intersection of two curves, the failure criterion and the load-rotation curve.

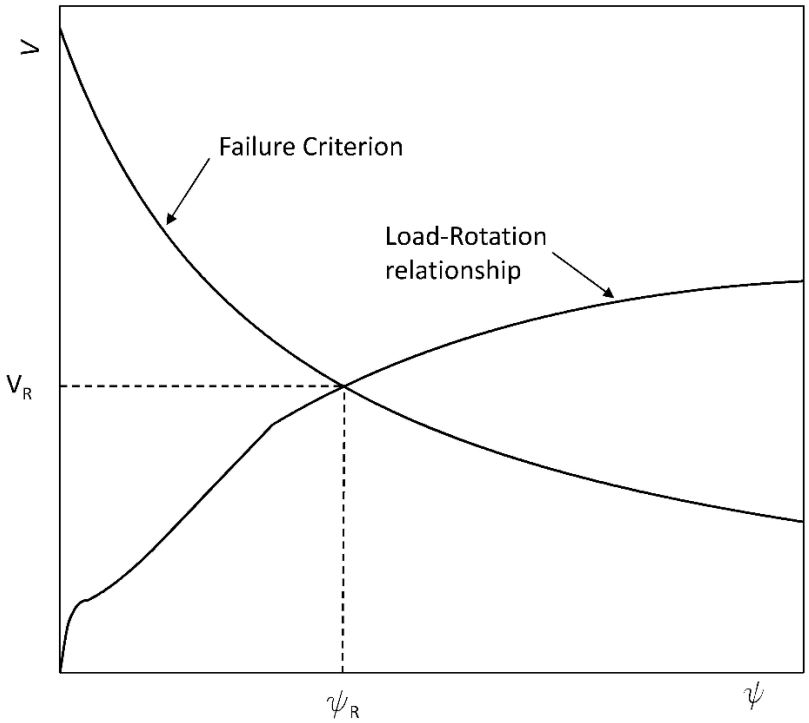

Figure 1 – Punching strength according to the CSCT (adapted from Muttoni [25])

Generally, the strengthening only affects the failure criterion or the load-rotation curve, nevertheless in some cases the strengthening may affect both curves as for the application of a bonded reinforced concrete overlay (BRCO) on the top of the slab.

3.2 Shear strengthening

Shear strengthening techniques could be classified according to types, arrangements and materials. The main types of shear reinforcements are listed in the following:

- anchored bolts with nut, washer and plate (Figure 2);
- headed bolts (Figure 2);
- bonded bolts (Figure 3);
- grids or fans (only for composite materials) (Figure 4);
- stirrups (only for composite materials) (Figure 5);

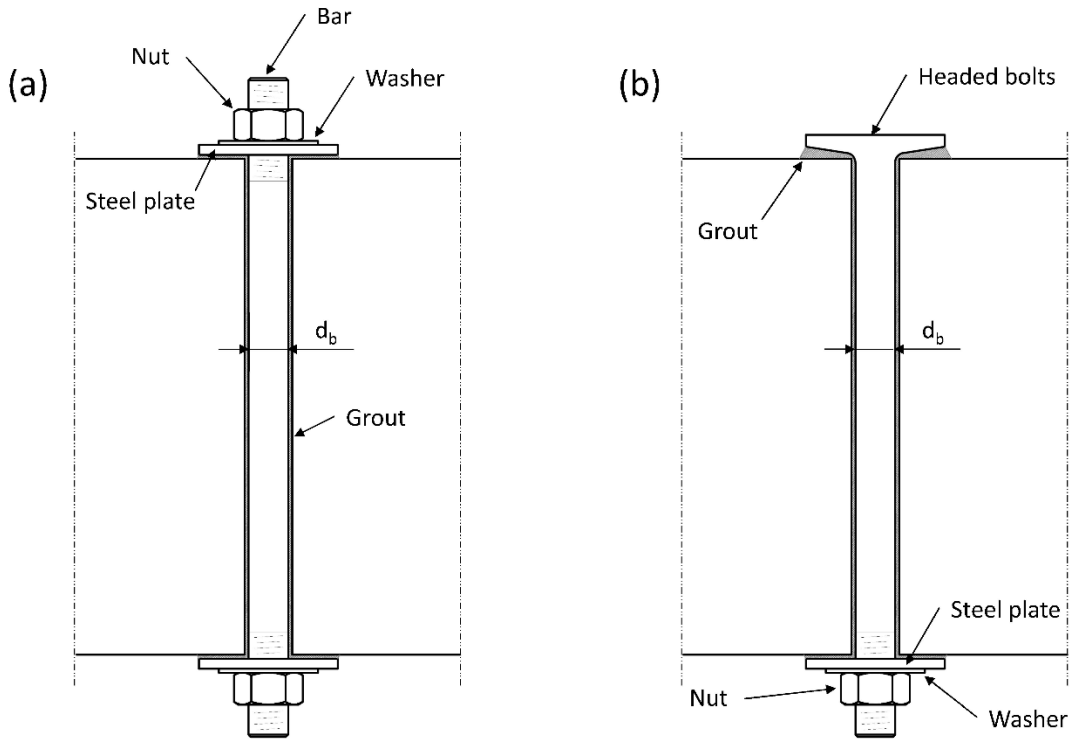

Figure 2 – (a) Anchored bolts with nut, washer and plate (b) headed bolts (adapted from El-Salakawi et al. [7])

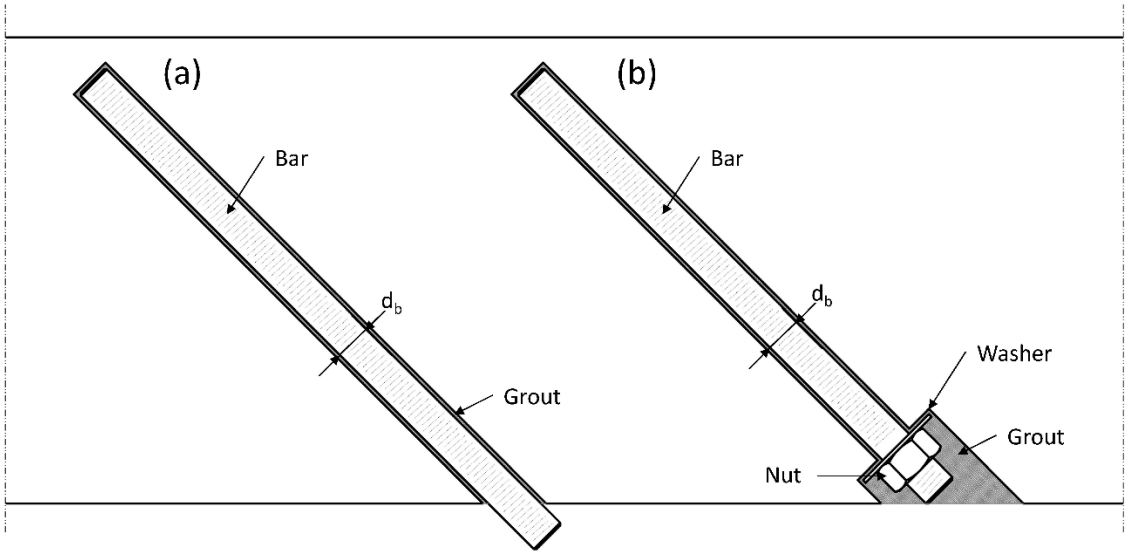

Figure 3 – (a) Bonded bolts without anchorages (adapted from Hassanzadeh [5]) (b) Bonded bolts anchored at the bottom (adapted from Ruiz et al. [37])

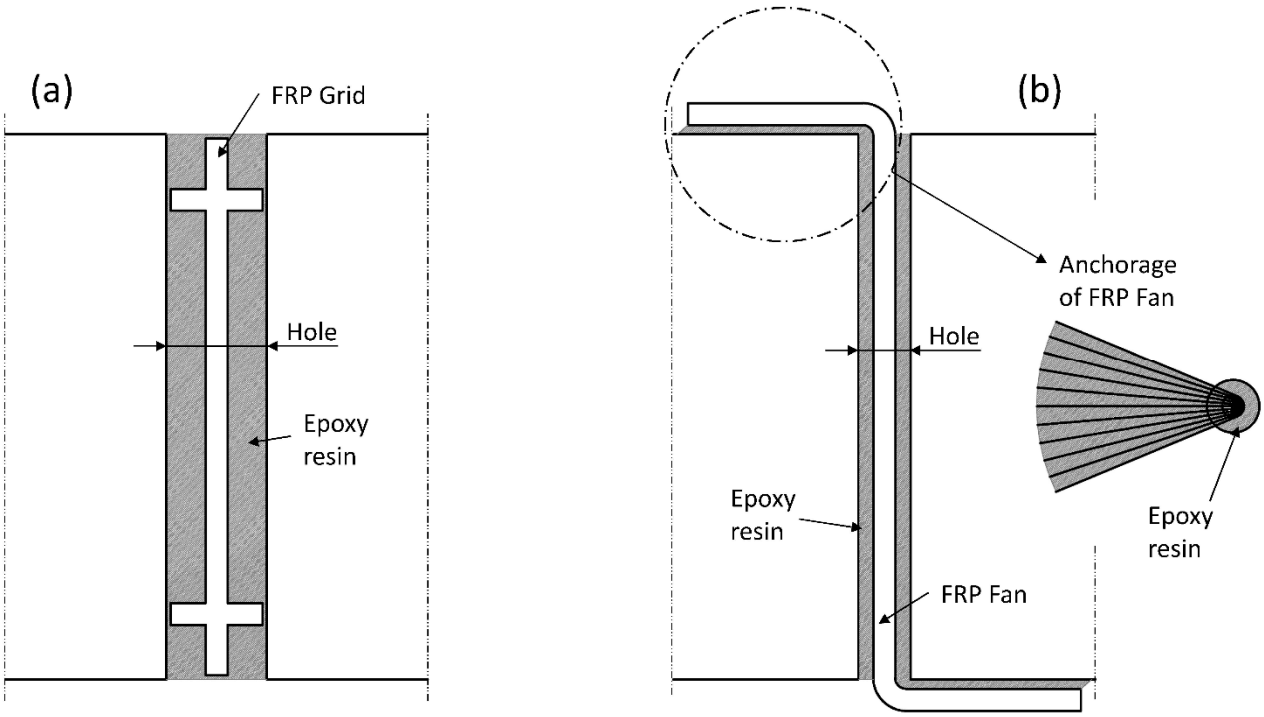

Figure 4 – (a) FRP grids (adapted from Meisami et al. [13]) (b) FRP fans (adapted from Meisami et al. [15])

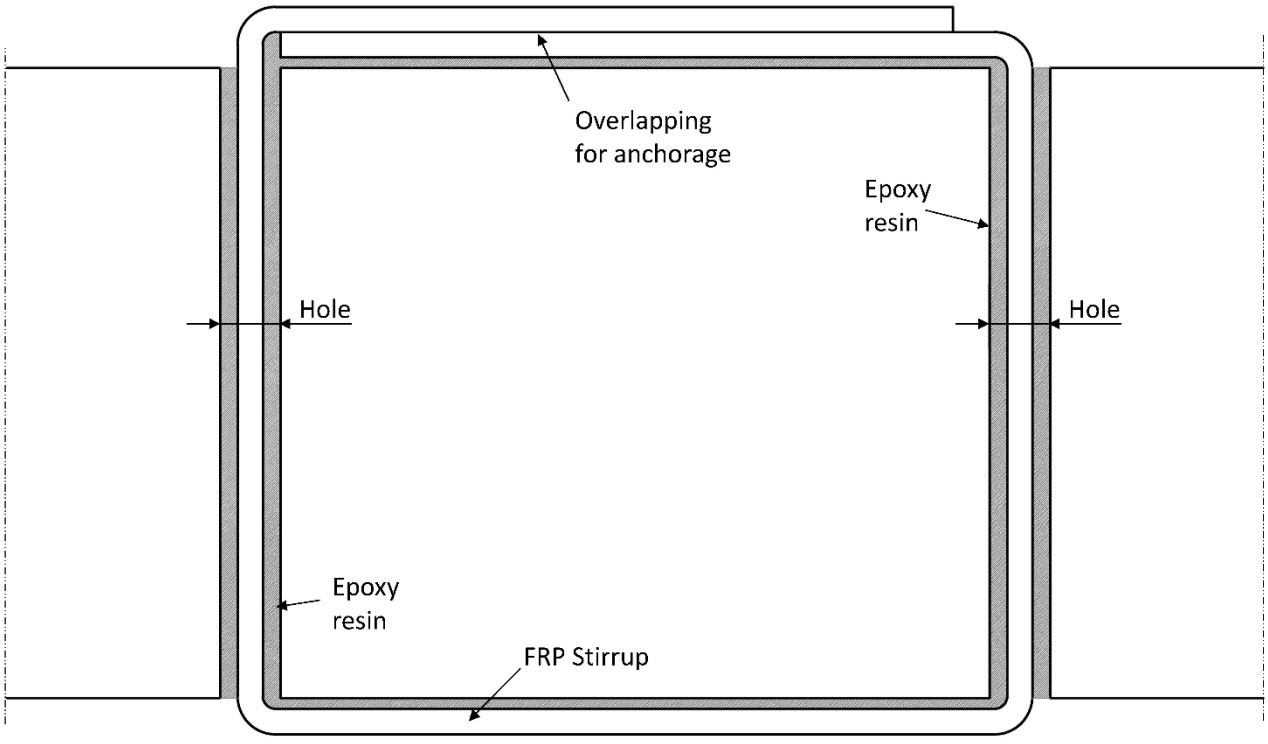

Figure 5 – FRP stirrups (adapted from Binici and Bayrak et al. [11])

The reinforcement arrangement could be radial or orthogonal (Figure 6). The main materials usually used in shear strengthening are: steel, CFRP and GFRP.

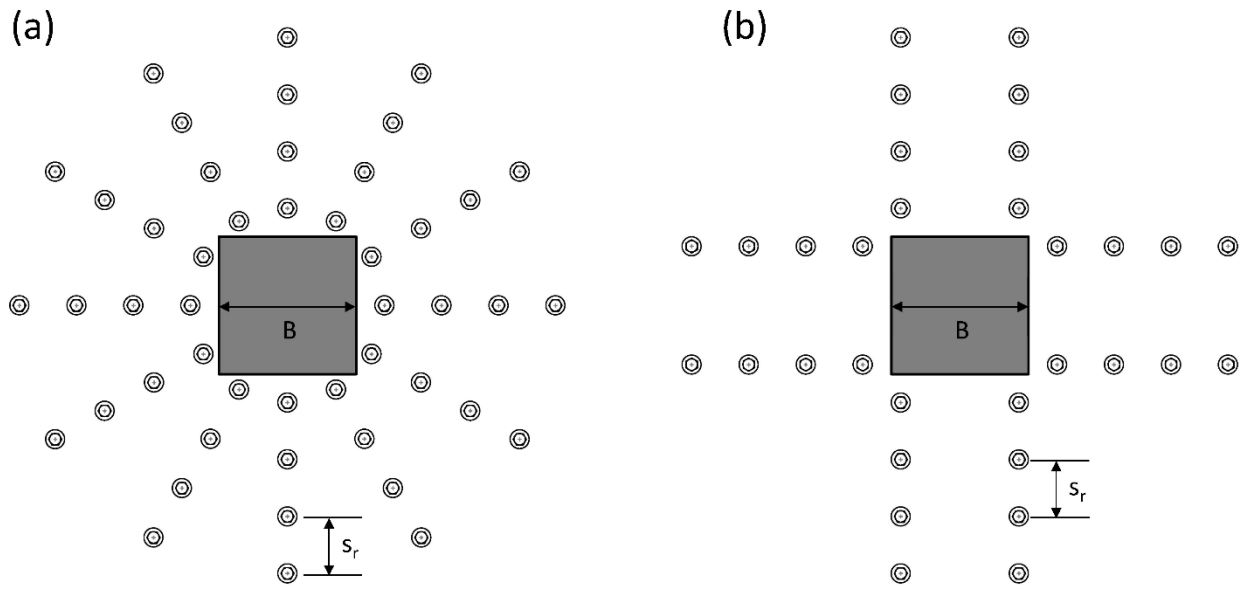

Figure 6 – Shear reinforcement arrangements: (a) radial arrangement (b) orthogonal arrangement

The installation of shear reinforcement enhances the punching strength. Applying the CSCT this effect could be explained by the raising of the failure criterion curve while the load-rotation curve is not affected by this type of strengthening (Figure 7).

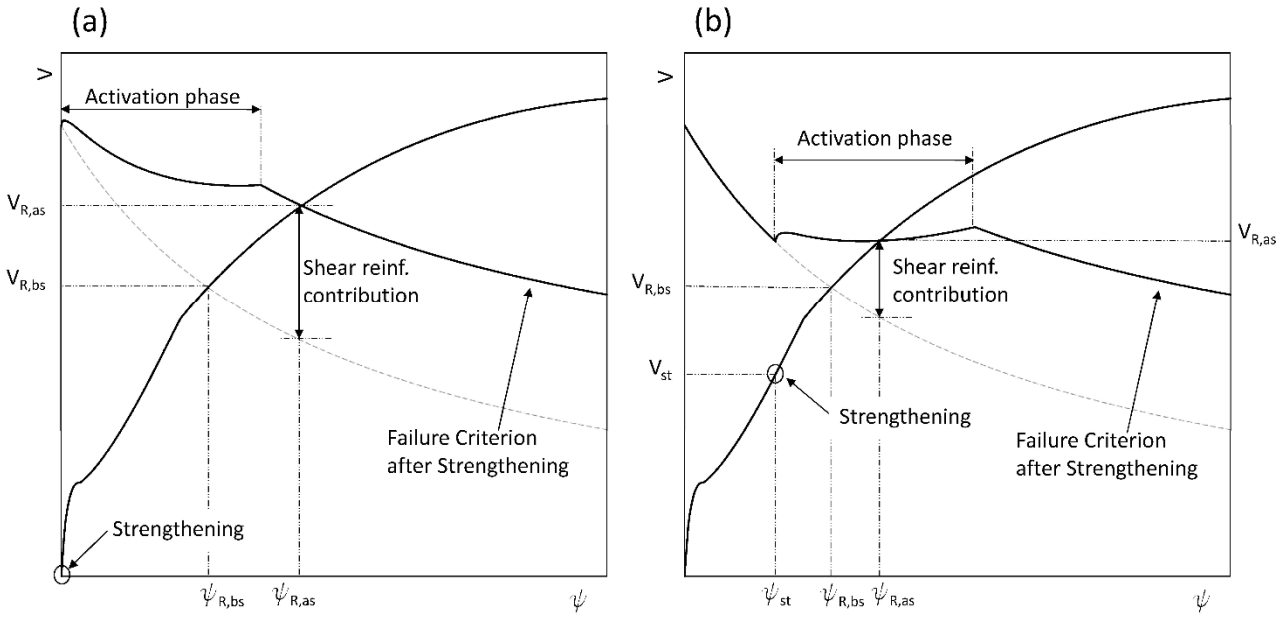

Figure 7 – Contribution of shear reinforcement to punching shear strength: (a) on unloaded slab (b) on loaded slab (adapted from Ruiz et al. [37])

As shown by Ruiz et al. [37] the effectiveness of shear strengthening is reduced by two facts: the first is the initial rotation of the slab due to service loading, the second is the activation phase of shear reinforcement. The initial rotation could be limited if the slab is unloaded by propping the structure, however as shown by Koppitz et al. [39] even in this case a residual rotation is still present (Figure 8). The amount of residual rotation depends on the maximum load level and the amount of flexural reinforcement. Usually the residual rotation is low and the punching strength after reloading is almost equal to the initial punching

strength, being the reduction more pronounced if the longitudinal reinforcement is yielded before unloading the slab [39].

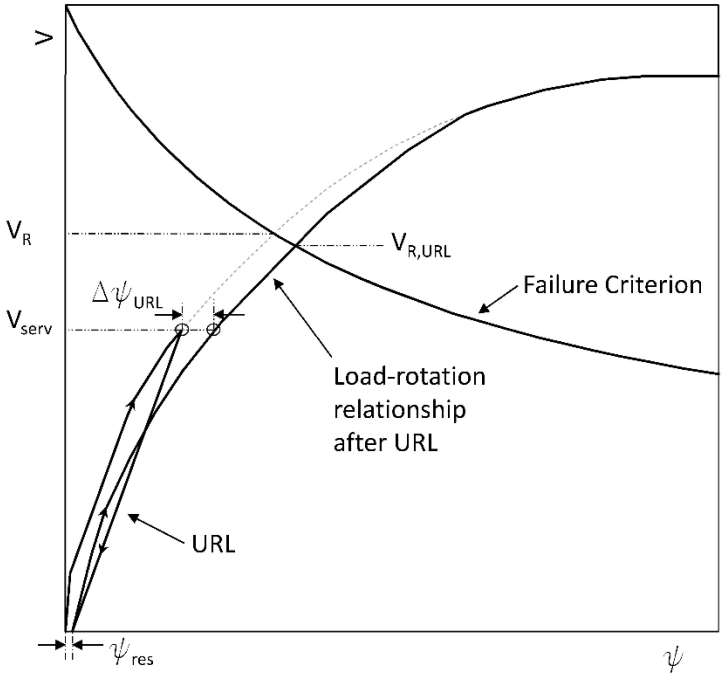

Figure 8 – Effect of unloading and reloading path on punching strength (adapted from Koppitz [40])

The activation phase is needed to load the reinforcement; the most effective technique to reduce this phase is prestressing the reinforcement. However, prestressing is not applicable to all types of reinforcement, so bolts and studs anchored at both ends are preferred. The punching strength after strengthening is given by Ruiz et al. [37] considering three types of failure (Figure 9):

$$V_{R,sr} = min\left(V_{R,in}; V_{R,crush}; V_{R,out}\right) \quad (1)$$

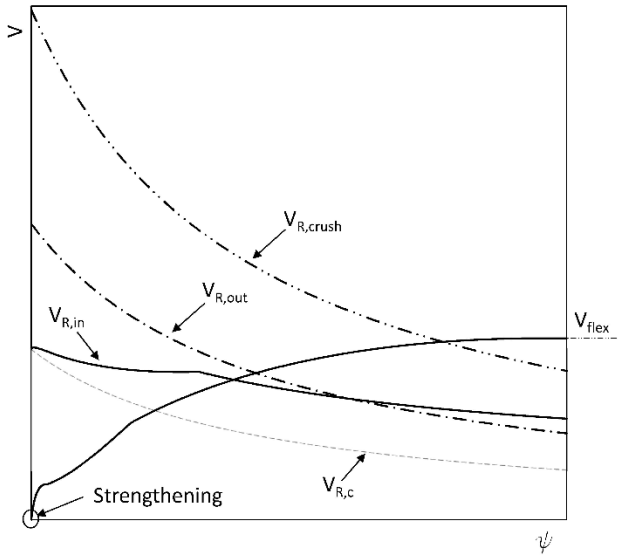

Figure 9 – Failure criterions of slabs strengthened with post-installed shear reinforcement

where $V_{R,in}$ is the punching within the shear reinforcement zone, $V_{R,crush}$ is the crushing of the concrete strut, $V_{R,out}$ is the punching outside the shear-reinforced zone. The punching strength within the shear reinforcement zone could be calculated as:

$$V_{R,in} = V_{R,c} + V_{R,s} \tag{2}$$

where $V_{R,c}$ and $V_{R,s}$ are the concrete and shear reinforcement contributions. $V_{R,c}$ is given by the following expression [25]:

$$V_{R,c} = \frac{3}{4} \cdot \frac{b_0 \cdot d \cdot \sqrt{f_c}}{1 + 15 \cdot \frac{\psi \cdot d}{d_{g0} + d_g}} \tag{3}$$

where d is the effective depth, b_0 is the control perimeter set at d/2 from the support, f_c is the concrete compression strength, d_g is the maximum diameter of the aggregate, d_{g0} is the reference aggregate size equal to 16 mm and ψ is the slab rotation. The shear reinforcement contribution could be calculated as [37]:

$$V_{R,s} = \sum_{i=1}^{n} \sigma_{si}(\psi) \cdot A_{swi} \cdot \sin(\beta_i) \tag{4}$$

where $\sigma_{si}(\psi)$ is the stress in reinforcement at the given rotation ψ, A_{swi} is the area of the bar and β_i is the angle of reinforcement.

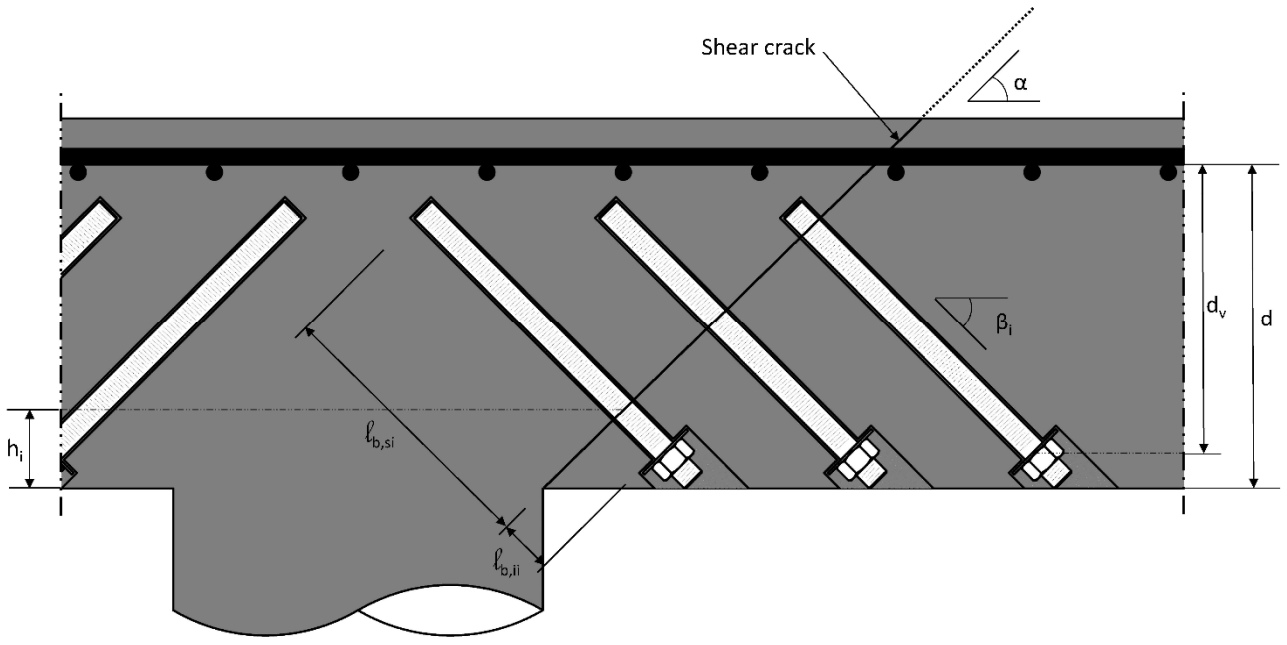

Figure 10 – Control shear parameters of bonded shear reinforcement anchored by the slab bottom (adapted from Ruiz et al. [37])

The stress in reinforcement $\sigma_{si}(\psi)$ increases as the crack opening w_b increases at the level of the bar, which is related with the slab rotation [37]:

$$w_b = 0.5 \cdot \psi \cdot h_i \cdot \cos\left(\alpha + \beta_i - \frac{\pi}{2}\right) \quad (5)$$

where the angle α of critical crack is assumed equal to π/4 [37] (Figure 10). For bonded reinforcement the activation phase is guaranteed by bond, instead for unbonded reinforcement it is only provided by the anchorage. Assuming a rigid-plastic law for bond, the bar stress during the activation phase can be calculated as [37]:

$$\sigma_{s,el} = \sqrt{\frac{4 \cdot \tau_b \cdot E_s \cdot w_b}{d_b}} \quad (6)$$

where τ_b is the bond strength, E_s is the elastic modulus of reinforcement and d_b is the bar diameter. For unbonded reinforcement the stress during the activation phase can be calculated as [41]:

$$\sigma_{s,el} = E_s \cdot \varepsilon_s + \sigma_{ps} = E_s \cdot \frac{w_b}{l_s} + \sigma_{ps} \quad (7)$$

where l_s is the length of the bar and σ_{ps} is the prestressing that could be applied to reduce the amplitude of the activation phase. The activation phase ends when the yielding stress (f_{yw}) is reached, then the contribution provided by reinforcement remains constant until failure (Figure 7). Actually as shown by Ruiz et al. [37] the failure could happen before the reinforcement yields for other reasons, so the stress should be calculated as:

$$\sigma_{si} = min(\sigma_{s,el}; \sigma_{s,b}; \sigma_{s,p}; f_{yw}) \quad (8)$$

where $\sigma_{s,b}$ is the stress that induces the failure by bond and $\sigma_{s,p}$ corresponds to the failure by pull-out of the anchorage. When the strengthening is performed from the bottom of the slab, as shown in Figure 10, the following equations could be used [37]:

$$\sigma_{s,b} = \frac{4 \cdot \tau_b \cdot l_{b,si}}{d_b} \quad (9)$$

$$\sigma_{s,p} = 19 \cdot \sqrt{f_c} \cdot \frac{l_{b,ii}^{1.5}}{d_b^2} \cdot \left(1 + \frac{d_{inf}}{l_{b,ii}}\right) \quad (10)$$

where d_{inf} is the diameter of the anchoring plate and the other symbols are shown in Figure 10. In case of bonded reinforcement without anchorages (Figure 3) the stress is calculated as σ_{si}=min($\sigma_{s,el}$; $\sigma_{s,b}$; f_{yw}) where $\sigma_{s,b}$ is provided by equation (9). In presence of double anchored reinforcement (Figure 2) the stress is calculated as σ_{si}=min($\sigma_{s,el}$; $\sigma_{s,p}$; f_{yw}) where $\sigma_{s,p}$ is provided by equation (10). In these cases $l_{b,si}$ and $l_{b,ii}$ should be substituted by min($l_{b,si}$; $l_{b,ii}$).

The crushing strength $V_{R,crush}$ of the concrete strut is highly affected by transverse strains, it could be calculated as [41]:

$$V_{R,crush} = \lambda \cdot \frac{3}{4} \cdot \frac{b_{0,col} \cdot d \cdot \sqrt{f_c}}{1 + 15 \cdot \frac{\psi \cdot d}{d_{g0} + d_g}} \quad (11)$$

where $b_{0,col}$ is the support perimeter and λ could be taken equal to 3 for well-anchored shear reinforcement [41], 2.6 for reinforcement anchored only on the bottom of the slab [37] and 2 for the other cases [41].

Outside the shear-reinforcement zone the shear strength could be assumed as [41]:

$$V_{R,out} = \frac{3}{4} \cdot \frac{b_{0,out} \cdot d_v \cdot \sqrt{f_c}}{1 + 15 \cdot \frac{\psi \cdot d_v}{d_{g0} + d_g}} \tag{12}$$

where d_v is the reduced effective depth.

The procedure described above is though for bonded reinforcement, anchored at the bottom of the slab [42], however it turned suitable for other types of shear reinforcement. Actually when the slab is available for strengthening on both top and bottom side, the use of double anchored reinforcement is suggested. Indeed, as mentioned above, prestressing the reinforcement allows for the activation phase to be reduced. Doing so the contribution of reinforcement becomes immediately available without any reduction. Furthermore, designing properly the anchorages it is possible to avoid the other types of failure, like the loss of bond between steel and concrete and the pull-out of the concrete cone. This aspect is also very important for designers, indeed the calculation of the failure by yielding of reinforcement is much easier than the others. Furthermore, it is affected by lower uncertainties compared to those required by the other type of failures, where several parameters come into play in the determination of the punching strength. Therefore, the use of anchored reinforcement provides advantages both in terms of strength and reliability.

The procedure is still valid for FRP reinforcement but the bond strength (τ_b) should be calibrated to the specific case, although the use of FRP shear-reinforcement is less appealing to strength existing reinforced concrete flat-slabs, than using steel reinforcement. Indeed with steel shear reinforcement, it is usually possible to shift the punching failure outside the reinforcement zone. In some cases, this is not possible due to the activation phase where the reinforcement is still elastic. For this reason the use of high strength materials is not required as the activation phase is governed by the slab rotation and by the elastic modulus of reinforcement and less by the strength. In Table 1 a comparison with experimental results is proposed.

Table 1 – Literature experimental results and comparison with CSCT; [1] type of reinforcement, *B+A* bonded reinforcement anchored at the bottom of the slab, *A* anchored reinforcement, *B* bonded reinforcement, *G* grids, *S* stirrups; [2] types of failure, *in* inside, *out* out-side, *crush* crushing of concrete strut, *flex* flexural failure.

Reference	Specimen	Material	Type[1]	f_c (MPa)	f_y (MPa)	f_{yw} (MPa)	ρ (%)	ρ_w (%)	n_r	n_a	Failure[2]	V_{exp} (kN)	V_{th} (kN)	V_{exp}/V_{th}
Binici et al. [11], [12]	A4-1	CFRP	S	28.3	448	876	1.76	0.88	8	4	out	596	610	0.98
	A4-2	CFRP	S	28.3	448	876	1.76	0.44	8	4	out	668	610	1.10
	A4-3	CFRP	S	28.3	448	876	1.76	0.22	8	4	in	618	610	1.01
	A4-4	CFRP	S	28.3	448	876	1.76	0.44	8	4	in	600	610	0.98
	A6	CFRP	S	28.3	448	876	1.76	0.66	8	6	out	721	685	1.05
	A8	CFRP	S	28.3	448	876	1.76	0.66	8	8	out	744	740	1.01
	B6	CFRP	S	28.3	448	876	1.76	0.44	8	4	out	756	610	1.24
	B6	CFRP	S	28.3	448	876	1.76	0.44	8	6	out	752	685	1.10
	B8	CFRP	S	28.3	448	876	1.76	0.44	8	8	out	778	740	1.05
Hassanz. [5]	SS1.s	steel	B	34.1	493	493	0.80	0.34	4	3	in	915	915	1.00
	SS3.s	steel	B	31.7	493	493	0.80	0.71	8	3	crush	935	982	0.95
Inácio et al. [8]	M6	steel	A	47.7	467	421	1.17	0.28	8	2	in	331	325	1.02
	M6S	steel	A	36.3	529	530	1.15	0.28	8	2	in	329	325	1.01
	M6SE	steel	A	26.8	529	530	1.04	0.28	8	2	in	274	290	0.94
	M8	steel	A	47.7	467	527	1.16	0.50	8	2	in	381	364	1.05
	M8a	steel	A	47.9	467	523	1.12	0.50	8	2	in	366	364	1.01
	M8S	steel	A	38.7	529	587	1.11	0.50	8	2	in	352	382	0.92
	M8SE	steel	A	26.8	529	587	1.04	0.50	8	2	in	273	330	0.83

	M10	steel	A	41.9	467	534	1.25	0.79	8	2	out	406	340	1.19
Meisami et al. [13], [14]	FR2-8	FRP	B	36.6	420	1400	1.10	0.80	4	2	out	248	219	1.13
	SN2-8	steel	A	37.7	420	320	1.10	1.31	4	2	flex	258	258	1.00
	FR3-8	FRP	B	43.5	420	1400	2.20	0.80	8	3	out	286	324	0.88
	FR3-24	FRP	B	43.5	420	1400	2.20	1.63	8	3	flex	412	366	1.13
	FG-8A	FRP	G	43.5	420	1400	2.20	0.16	4	2	in	314	300	1.05
	FG-16A	FRP	G	44.1	420	1400	2.20	0.32	8	2	out	348	361	0.96
	FG-24A	FRP	G	41.7	420	1400	2.20	0.32	8	3	in	375	371	1.01
Ruiz et al. [37]	PV2	steel	B+A	35.4	709	574	1.5	0.47	8	3	in	1383	1320	1.05
	PV3	steel	B+A	35.6	709	574	1.5	0.95	12	3	out	1577	1447	1.09
	PV6	steel	B+A	33.3	505	574	0.57	0.62	8	4	flex	850	827	1.03
	PV7	steel	B+A	33.8	505	574	0.57	0.62	8	4	flex	854	828	1.03
	PV8	steel	B+A	34.1	505	574	0.57	0.31	4	4	flex	833	827	1.01
	PV14	steel	B+A	36.6	527	574	1.5	1.14	12	6	crush	1690	1517	1.11
	PV15	steel	B+A	36.8	527	574	1.5	0.95	12	6	crush	1609	1519	1.06
	PV16	steel	B+A	37.2	527	574	1.5	0.35	6	4	in	1263	1195	1.06
	PV17	steel	B+A	29.9	518	574	1.5	0.24	4	4	in	1121	1040	1.08
	PV18	steel	B+A	28.2	518	574	1.0	0.35	6	4	in	1070	1013	1.06
	PV19	steel	B+A	29.2	518	574	1.0	0.24	4	4	in	1075	919	1.17
													Avg	1.036
													CoV	0.078

where n_r is the number of radii of shear reinforcement, n_a is the number of shear reinforcement per radius and ρ_w is the shear reinforcement ratio calculated according to:

$$\rho_w = \frac{n_r \cdot \frac{\pi}{4} \cdot d_b^2}{s_r \cdot b_0} \tag{13}$$

being s_r the distance between two consecutive radii. As shown in Table 1, when ρ_w is greater than 0.5%, the failure is usually shifted outside the shear reinforcement zone. However, the punching strength is limited by crushing of the concrete strut or by flexural failure.

3.3 Flexural strengthening

Flexural strengthening usually can be achieved by adding longitudinal reinforcement on the top of the slab, for example gluing FRP strips in both orthogonal directions or using a bonded reinforced concrete overlay (BRCO).

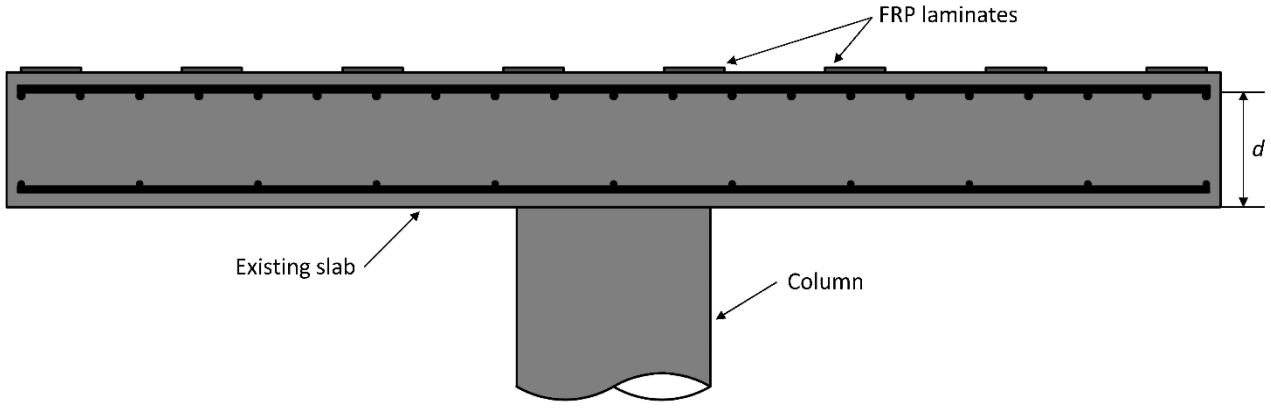

Figure 11 – Cross-section of a strengthened slab with FRP strips (adapted from Faria et al. [24])

Using glued FRP strips in both orthogonal directions as a strengthening technic only affects the load-rotation curve, while the failure criterion remains almost the same. The load-rotation curve after strengthening becomes stiffer since the amount of longitudinal reinforcement is increased. Also in this case, like in shear strengthening, the initial rotation reduces the effectiveness of the strengthening (Figure 12).

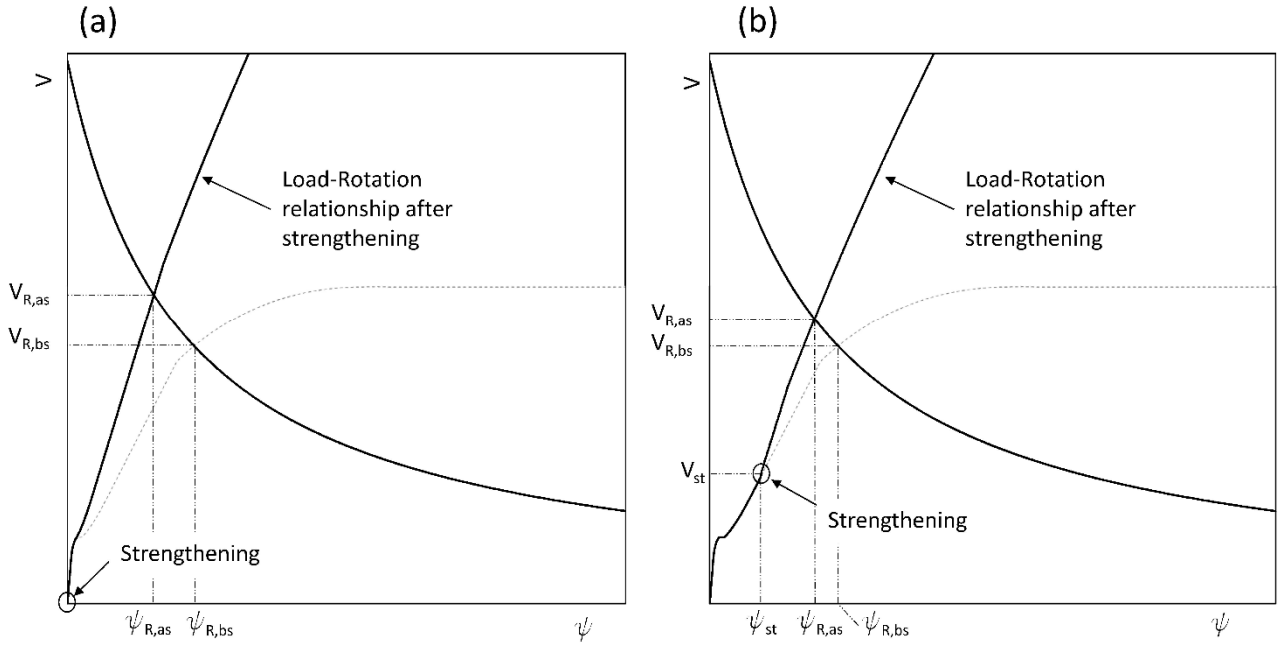

Figure 12 – Load-rotation curve and failure criterion of strengthened slab with FRP strips: (a) on unloaded slab (b) on loaded slab

Generally this strengthening technique increases the punching strength, but reduces the ductility of the connection. The failure becomes more brittle since the ultimate rotation after strengthening is lower than that of the existing slab. The effectiveness of this strengthening technique is strictly related to the amount of flexural reinforcement of the existing slab. For low reinforcement ratios (ρ<0.5%) when the failure is usually governed by flexure, the strengthening is effective; for high reinforcement ratios (ρ >1 %), when the failure is usually governed by punching, the effectiveness of the strengthening is lower [24] and in some cases the increase of punching capacity is even lower than 10% [19] [43]. Actually, Chen and Li [20] shown high increase in punching strength even in presence of large amount of flexural reinforcement (ρ=1.31 %). However, this apparent contradiction is explained by the small effective depth (≈70 mm) of slabs tested by Chen and Li [20].

Following Faria et al. [24] the installation of FRP strips could be taken into account by introducing an equivalent longitudinal reinforcement ratio:

$$\rho_{eq} = \frac{a_s + a_{s,st} \cdot \frac{E_{st}}{E_s} \cdot \frac{d_{st}}{d}}{d} \tag{14}$$

where a_s and a_{st} are the cross-sectional areas per unit width of the longitudinal reinforcement and FRP, respectively.

In Table 2 results of the application of FRP to existing slabs are presented. The strengthening is performed on 250 mm thick slabs at varying the longitudinal reinforcement ratio (ρ). Both CFRP tissues and laminates are considered, in the second case the spacing of strips is set equal to 400 mm, equal to the cross-section

side of the square column. The concrete strength and the yielding stress are assumed equal to 28 MPa and 450 MPa, respectively.

Table 2 – Strengthening with FRP: CSCT prediction of punching strength after strengthening; *strengthening performed on unloaded slab, **strengthening performed on loaded slab $V_{st}=50\%\cdot V_R$

Type	h (mm)	d (mm)	a_s (mm^2/mm)	ρ (%)	E_{st} (GPa)	d_{st} (mm)	a_{st} (mm^2/mm)	$f_{u,st}$ (MPa)	ρ_{eq} (%)	$V_{R,bs}$ (kN)	$V_{R,as}$ * (kN)	ΔR * (%)	$V_{R,as}$ ** (kN)	ΔR ** (%)
1 CFRP tissue, (1000 g/m^2)	250	209	1.05	0.50	210	250	0.546	2800	0.83	707	905	28%	827	17%
	250	209	1.57	0.75	210	250	0.546	2800	1.08	876	1000	14%	914	4%
	250	209	2.09	1.00	210	250	0.546	2800	1.33	965	1050	9%	995	3%
	250	209	2.61	1.25	210	250	0.546	2800	1.58	1021	1100	8%	1050	3%
2 CFRP tissues, (2000 g/m^2)	250	209	1.05	0.50	210	250	1.092	2800	1.16	707	1005	42%	901	27%
	250	209	1.57	0.75	210	250	1.092	2800	1.41	876	1055	20%	969	11%
	250	209	2.09	1.00	210	250	1.092	2800	1.66	965	1100	14%	1027	6%
	250	209	2.61	1.25	210	250	1.092	2800	1.91	1021	1130	11%	1079	6%

As shown in Table 2 the effectiveness of the strengthening decreases at increasing the longitudinal reinforcement ratio of the existing slab. The effectiveness is further reduced when the strengthening is performed on loaded slabs (Vst≠0).

When the strengthening with FRP is not enough to achieve the design punching capacity, a bonded reinforced concrete overlay (BRCO) could be used. The application of a BRCO (Figure 13) could be included in the flexural strengthening techniques, but actually it affects both the load rotation curve and the failure criterion. This technique allows for increase the punching strength thanks to the enhancing of the failure criterion curve.

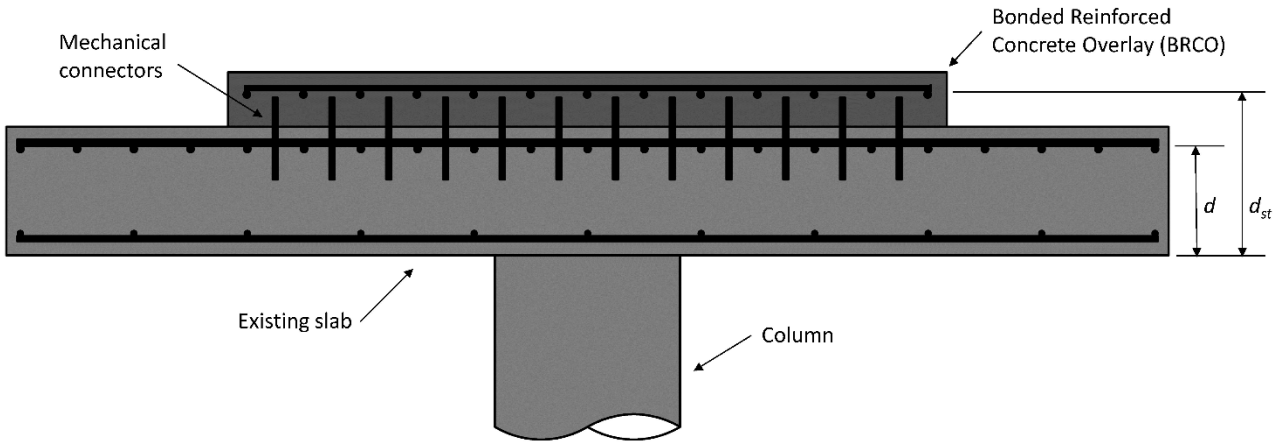

Figure 13 – BRCO

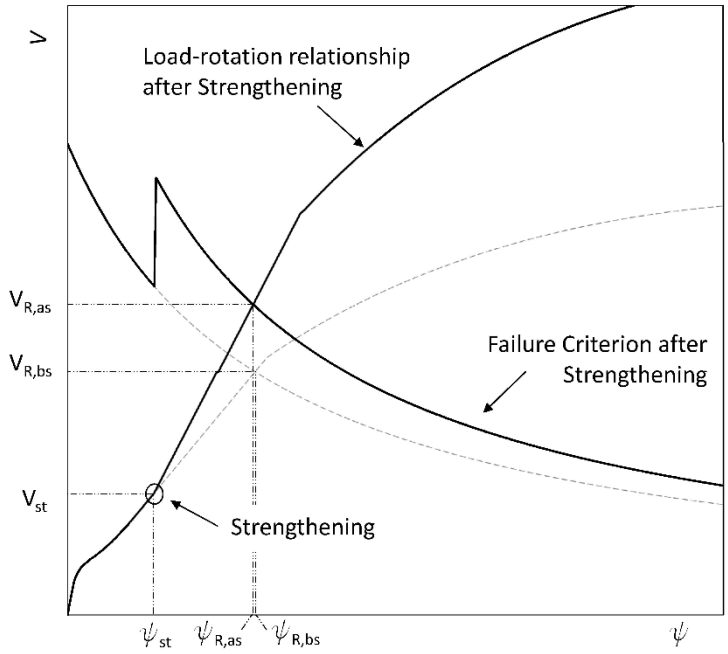

Figure 14 – Load-rotation curve and failure criterion of strengthened slab with BRCO

As shown by Lapi et al. [36] this technique is effective even if it is applied to loaded slabs (V_{st}=50%·V_R) with high reinforcement ratio (ρ=2%). In this case the increase of punching strength ΔR after strengthening is even greater than 20%.

Table 3 – Strengthening with BRCO: CSCT prediction of punching strength after strengthening; **strengthening performed on loaded slab V_{st}=50%·V_R

Type	h (mm)	d (mm)	a_s (mm²/mm)	ρ (%)	h_{st}-h (mm)	d_{st} (mm)	a_{st} (mm²/mm)	ρ_{eq} (%)	$V_{R,bs}$ (kN)	$V_{R,as}$** (kN)	ΔR** (%)
BRCO Ø12/150	220	175	0.875	0.50	50	235	0.754	1.08	475	770	62%
	220	175	1.75	1.00	50	235	0.754	1.58	685	920	34%
	220	175	2.625	1.50	50	235	0.754	2.08	800	995	24%
	220	175	3.50	2.00	50	235	0.754	2.58	855	1060	24%
BRCO Ø14/150	220	175	0.875	0.50	50	235	1.026	1.29	475	815	72%
	220	175	1.75	1.00	50	235	1.026	1.79	685	945	38%
	220	175	2.625	1.50	50	235	1.026	2.29	800	1020	28%
	220	175	3.50	2.00	50	235	1.026	2.79	855	1075	26%
BRCO Ø16/150	220	175	0.875	0.50	50	235	1.340	1.53	475	855	80%
	220	175	1.75	1.00	50	235	1.340	2.03	685	975	42%
	220	175	2.625	1.50	50	235	1.340	2.53	800	1040	30%
	220	175	3.50	2.00	50	235	1.340	3.03	855	1090	27%

As shown in Table 3 the application of a BRCO appears an efficient strengthening solution for punching. However the use of mechanical connectors is highly recommended to prevent the premature debonding of the overlaid concrete. The failure criterion after strengthening was provided by Lapi et al. [36] and can be calculated as:

$$V_{R,brco} = \frac{3}{4} \cdot \frac{b_{0,st} \cdot d_{st} \cdot \sqrt{f_c}}{1 + 15 \cdot \frac{\psi \cdot d_{st}}{d_{g0} + d_g}} \tag{15}$$

where d_{st} is the effective depth of the strengthened slab and $b_{0,st}$ is the control perimeter set at d_{st}/2 from

the support. The stiffer behavior of the load rotation curve after strengthening is due to the insertion of flexural reinforcement on the top of the slab. According to the CSCT [25] the load-rotation curve is built starting from the slab rotation (ψ) and the quadrilinear moment-curvature relationship (m, χ), writing the equilibrium equation for a sector of slab. The application of the CSCT to strengthened slabs requires some modifications in the moment-curvature relationship. When the strengthening is performed on loaded slabs three cases may be distinguished [36] (Figure 15):

- strengthening during the elastic phase of the section (curve b);
- strengthening during the cracked phase of the section (curve c);
- strengthening at the yielding plateau (curve d);

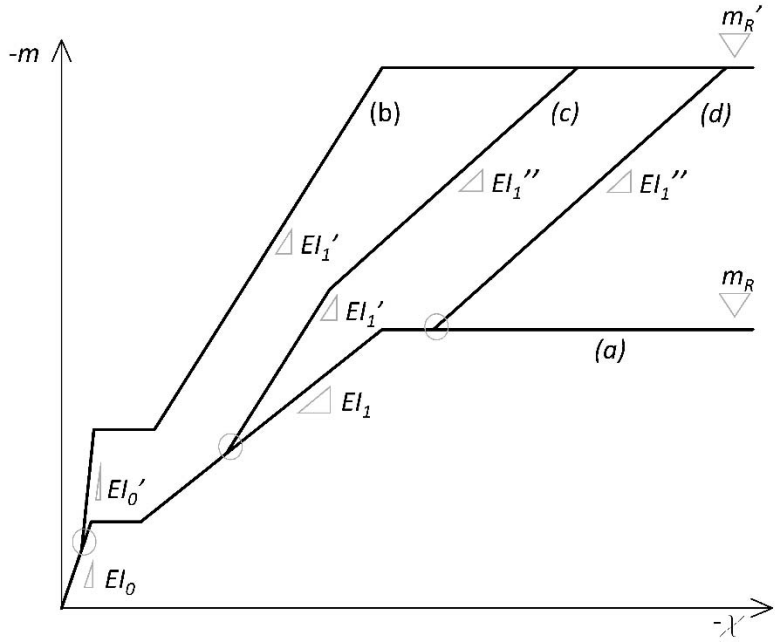

Figure 15 – Moment-curvature relationships: curve labelled (a) un-strengthened slab; (b) strengthening during the elastic phase; (c) strengthening during the cracked phase; (d) strengthening at the yielding plateau

In analogy with the formulation proposed by Muttoni [25] the stiffness of the strengthened section before cracking is:

$$EI_0' = \frac{E_c \cdot h_{st}^3}{12} \tag{16}$$

while in the cracked phase, before yielding of longitudinal reinforcement, becomes:

$$EI_1' = \beta \cdot E_s \cdot \left[\rho \cdot d^3 \cdot \left(1 - \frac{c'}{d}\right) \cdot \left(1 - \frac{c'}{3 \cdot d}\right) + \rho_{st} \cdot d_{st}^3 \cdot \left(1 - \frac{c'}{d_{st}}\right) \cdot \left(1 - \frac{c'}{3 \cdot d_{st}}\right)\right] \tag{17}$$

where β is the efficiency factor [25] and c' is the compressive depth of the strengthened section before yielding of existing reinforcement (Figure 16).

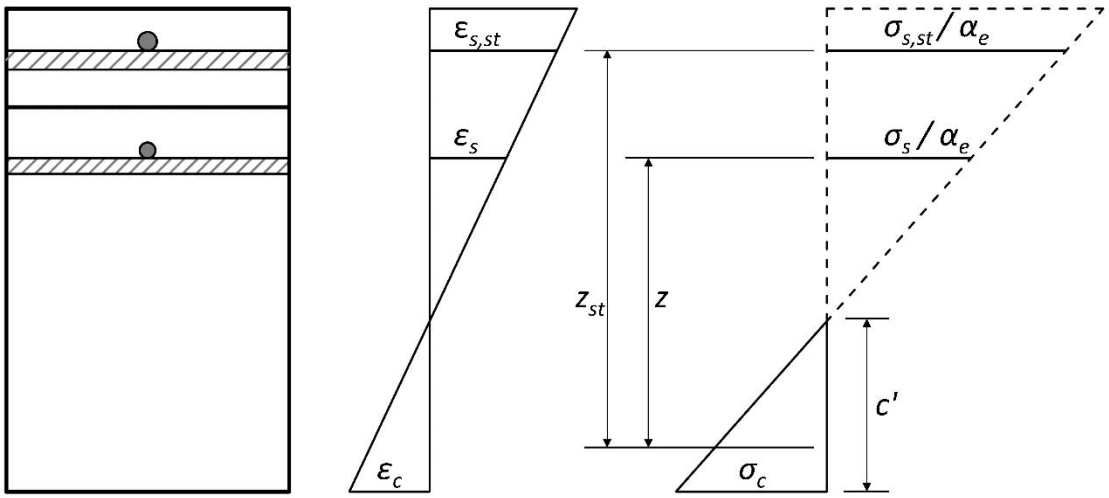

Figure 16 – Strains and stresses during the cracked phase of strengthened section ($\alpha_e=E_s/E_c$)

The stiffness of the strengthened section in the cracked phase, after yielding of longitudinal reinforcement, becomes:

$$EI_1'' = \beta \cdot E_s \cdot \rho_{st} \cdot d_{st}^3 \cdot \left(1 - \frac{c''}{d_{st}}\right) \cdot \left(1 - \frac{c''}{3 \cdot d_{st}}\right) \tag{18}$$

where c'' is the compressive depth after yielding of the existing reinforcement. Finally, the ultimate moment becomes:

$$m'_R = \rho \cdot d \cdot f_y \cdot \left[d - \frac{(0.8 \cdot c_u)}{2}\right] + \rho_{st} \cdot d_{st} \cdot f_{y,st} \cdot \left[d_{st} - \frac{(0.8 \cdot c_u)}{2}\right] \tag{19}$$

where $f_{y,st}$ is the yielding strength of rebars placed in the BRCO and c_u is the compressive depth of the strengthened section at ultimate state. More information about the load-rotation curve of the strengthened slab are found in Lapi et al. [36]. In Table 4 a comparison with the experimental results is proposed:

Table 4 – Main properties of literature experimental results and comparison with CSCT

Reference	Specimen	h (mm)	h_{BRCO} (mm)	f_c (MPa)	f_y (MPa)	d (mm)	d_{st} (mm)	a_s (mm^2/mm)	a_{st} (mm^2/mm)	V_{exp} (kN)	V_{th} (kN)	V_{exp}/V_{th}
Fernandes et al. [34]	STC	150	60	21.1	532	109	175	2.01 (ϕ16/10)	1.57 (ϕ10/10)	568	538	0.98
	STANC	150	60	20.5	532	109	175	2.01 (ϕ16/10)	1.57 (ϕ10/10)	550	535	1.03
											Avg	1.00

As shown in Table 5 the results in term of punching strength provided by the proposed method are aligned with those of the experimental results.

3.4 Enlargement of the support

The enlargement of the support could be improved by widening the column, casting a concrete capital or post-installing a steel capital (Figure 17). The two last solutions can be treated like the first if the failure

does not affect the capital. Furthermore, the capital should be sufficiently stiff to give adequate support to the slab, otherwise the efficacy of the strengthening could be impaired.

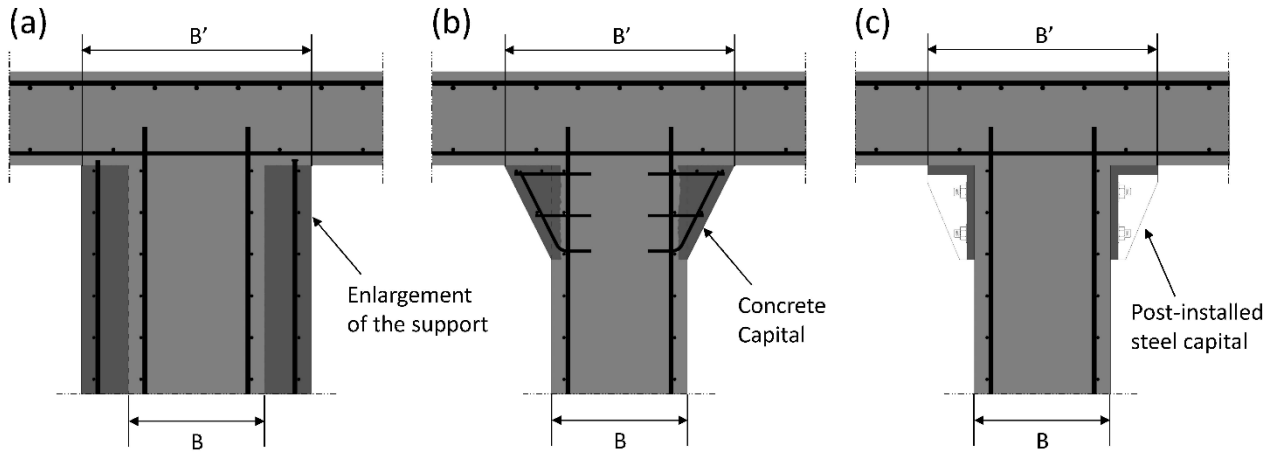

Figure 17 – Strengthening of flat-slab by enlargement of the support: (a) column widening; (b) casting new concrete capital; (c) post-installing steel capital (adapted from Hassanzadeh [5]).

Following the CSCT [25] the enlargement of the support affects both the failure criterion curve and the load-rotation curve (Figure 18). However, the modification of the load-rotation curve is only found near the horizontal plateau where the ultimate flexural capacity is achieved. For this reason this strengthening technique, unlike others, is not much affected by the initial rotation.

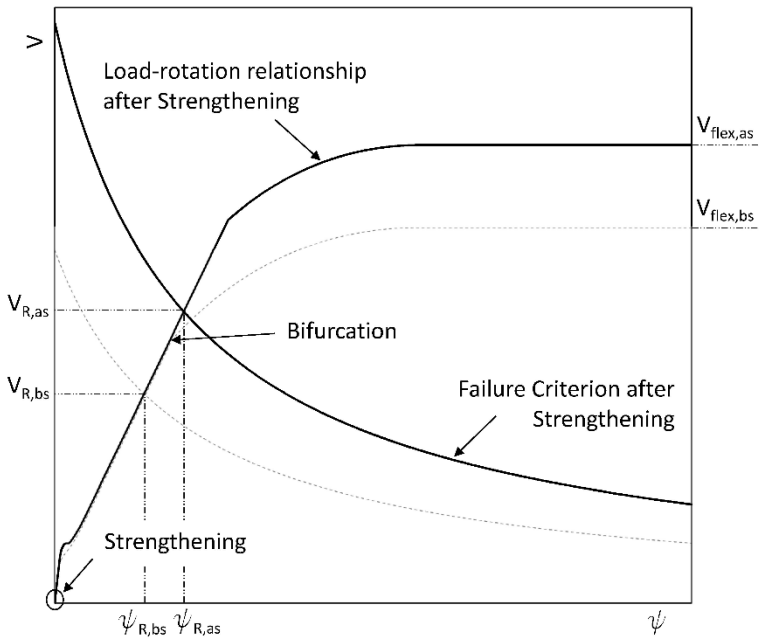

Figure 18 – Load-rotation curve and failure criterion of strengthened by enlargement of the support

The increase of the failure load is provided by the increase of the critical perimeter after strengthening. As shown by Hassanzadeh [5] the new punching strength could be calculated considering the support size after strengthening, as for a new column with the same perimeter:

$$V_{R,enl} = \frac{3}{4} \cdot \frac{b_{0,st} \cdot d \cdot \sqrt{f_c}}{1 + 15 \cdot \frac{\psi \cdot d}{d_{g0} + d_g}} \quad (20)$$

where $b_{0,st}$ is the control perimeter set at d/2 from the enlarged support. Actually when the strengthening is performed on loaded slabs (ψ_{st}; V_{st}), equation (21) should be modified to account for a reduced slab rotation ($\psi' = \psi - \psi_{st}$). Indeed, before strengthening the critical crack develops from the perimeter of the support, while after strengthening the first crack stops and another crack, placed on the perimeter of the capital, begins to open. However there are no experimental evidences about the strengthening of loaded slabs by enlarging the support, therefore the use of ψ is preferred to ψ' since the former provides results on the safe side.

The modification of the load-rotation curve is provided by the increase in flexural capacity due to the enlargement of the support. For an axisymmetric isolated slab (Figure 19), loaded on the perimeter, the flexural capacity could be calculated as:

$$V_{flex} = \frac{2 \cdot \pi \cdot m_R \cdot r_s}{r_s - r_c} \quad (21)$$

where r_s is the radius of the isolated slab (for continuous slabs could be assumed r_s=0.22·L [25] where L is the span of the slab) and r_c is the radius of the support. As highlighted by equation (21) the slab flexural capacity increases at decreasing the support size ($2 \cdot r_c$).

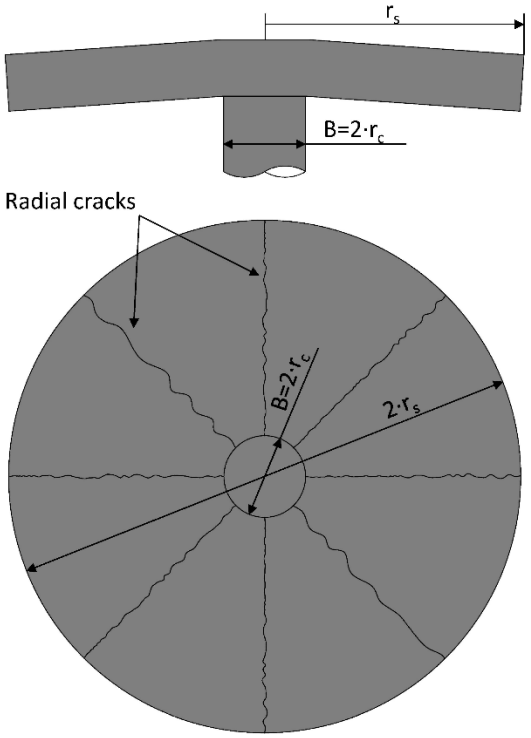

Figure 19 – Assumed flexural failure mechanism for circular isolated slab

In Table 5 the results of the strengthening by enlargement of the support are presented. The strengthening is performed on 250 mm thick slabs at varying the longitudinal reinforcement ratio (ρ). Both 300x300 mm and 400x400 mm column sizes are considered. The concrete strength and the yielding stress are assumed equal to 28 MPa and 450 MPa, respectively. Finally, the enlargement size is assumed equal to two times the existing column size (B'=2·B).

Table 5 – Strengthening against punching by enlarging the support: CSCT prediction of punching strength after strengthening; **strengthening performed on loaded slab with $V_{st} \leq 50\% \cdot V_R$

h (mm)	d (mm)	B (mm)	B' (mm)	b_0 (mm)	$b_{0,st}$ (mm)	$b_{0,st}/b_0$	ρ (%)	$V_{R,bs}$ (kN)	$V_{R,as}$** (kN)	ΔR** (%)
250	209	300	600	1857	3057	1.65	0.50	641	850	33%
250	209	300	600	1857	3057	1.65	0.75	774	1078	39%
250	209	300	600	1857	3057	1.65	1.00	854	1200	41%
250	209	300	600	1857	3057	1.65	1.25	900	1268	41%
250	209	300	600	1857	3057	1.65	1.50	950	1313	38%
250	209	400	800	2257	3857	1.71	0.50	707	1000	41%
250	209	400	800	2257	3857	1.71	0.75	876	1300	48%
250	209	400	800	2257	3857	1.71	1.00	965	1401	45%
250	209	400	800	2257	3857	1.71	1.25	1021	1500	47%
250	209	400	800	2257	3857	1.71	1.50	1100	1562	42%

As shown in Table 5 the enlargement of the support represents an efficient strengthening technique against punching; unlike other techniques it is not much affected by the amount of flexural reinforcement of the existing slab. The main variable is the size of the critical perimeter after strengthening ($b_{0,st}$) and in particular the ratio between the critical perimeter after and before strengthening ($b_{0,st}/b_0$). The punching strength after strengthening could be estimated approximately as:

$$V_{R,as} \cong V_{R,bs} \cdot \frac{b_{0,st}}{b_0} \tag{22}$$

Actually, the latter always leads to overestimate the punching capacity after strengthening (see Table 5). Equation (22) would be correct if the load-rotation curve was vertical, actually as it is inclined, the punching capacity after strengthening is always lower than equation (22) (Figure 18). In Table 6 a comparison with the experimental results is proposed.

Reference	Specimen	Type[1]	B (mm)	B' (mm)	b_0 (mm)	$b_{0,st}$ (mm)	d (mm)	f_c (MPa)	f_y (MPa)	ρ (%)	V_{exp} (kN)	V_{th} (kN)	V_{exp}/V_{th}
Hassanz. [5]	SS2.k	C	250	750	1414	2985	200	33.8	493	0.80	1190	1200	0.99
	SS4.k	C	250	500	1414	2199	199	31.5	493	0.80	950	944	1.01
	SS5.p	S	250	636	1414	2628	199	26.3	493	0.80	1008	990	1.02
Widianto [27]	RcG0.5	S	407	813	2025	3650	127	31.9	455	0.50	451	424	1.06
	RcG1.0	S	407	813	2025	3650	127	28.1	455	1.00	569	550	1.04
												Avg	1.024
												CoV	0.026

Table 6 – Main properties of literature experimental results and comparison with CSCT; 1 type of support enlargement: *C* concrete capital, *S* steel capital.

Values of the punching strength provided by the proposed method are in accordance with the experimental failure loads.

3.5 Post-tensioning

Finally, post-tensioning systems are also available to strength existing R/C flat-slabs. These strengthening techniques could be grouped to two categories: flexural strengthening and shear strengthening. The first is usually performed installing and prestressing FRP strips on the top of the slab (Figure 20).

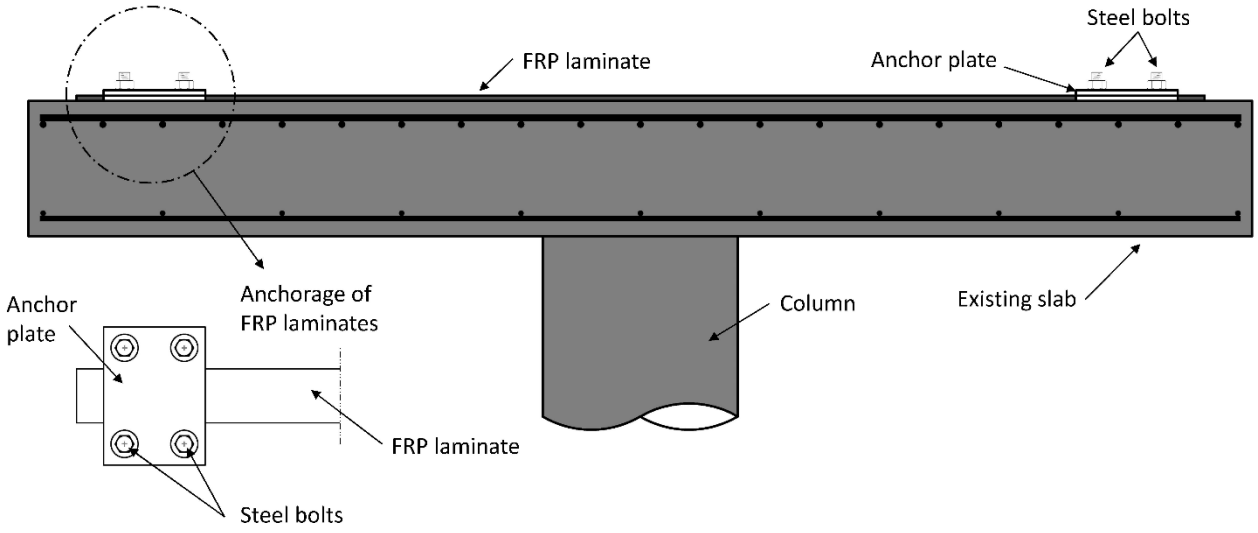

Figure 20 – prestressing system for flexural strengthening: FRP strips and anchor plate (adapted from Abdullah et al. [22])

The second is performed with inclined steel or FRP straps anchored through steel plates or by bonding; the second has been tested only for steel tendons (Figure 21).

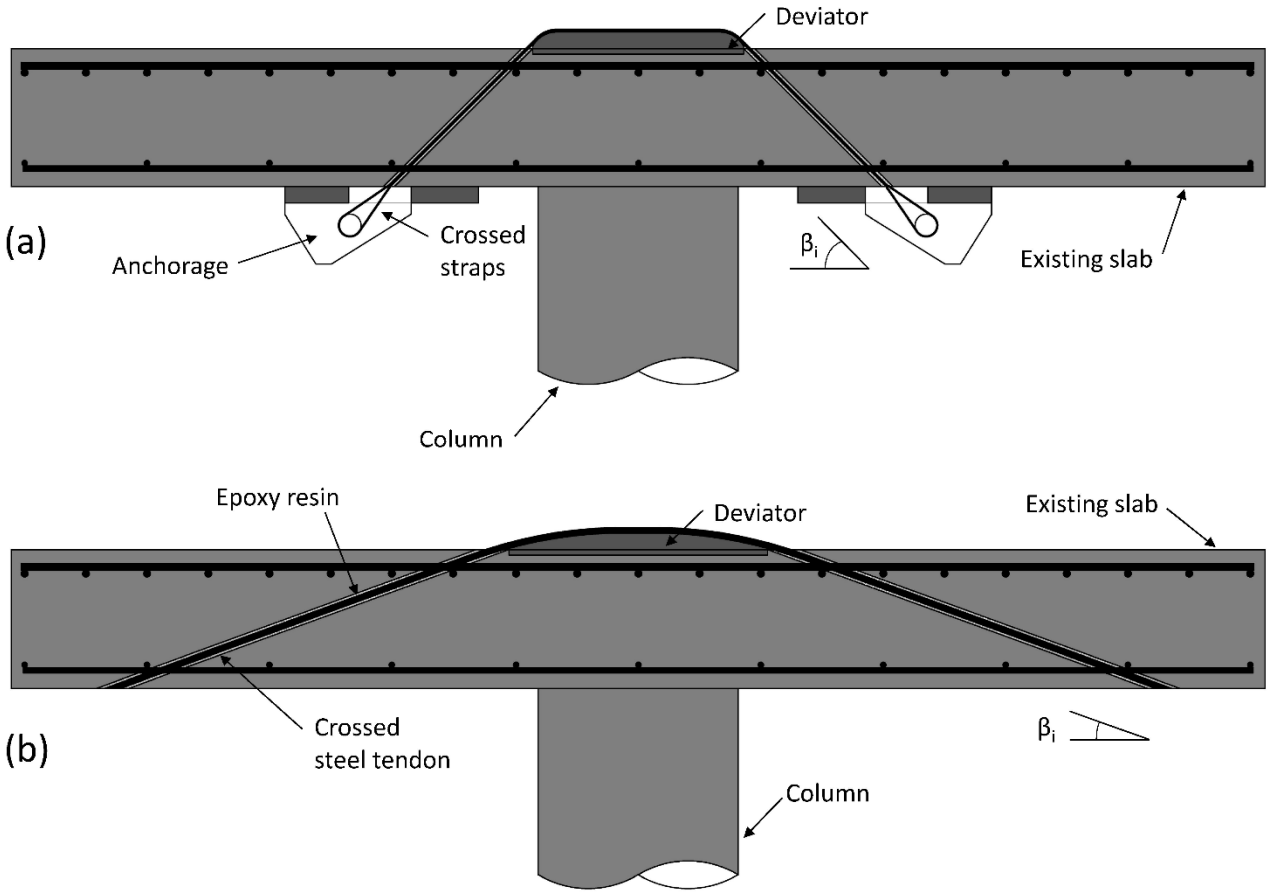

Figure 21 – prestressing system for shear strengthening: (a) CFRP straps anchored with steel plates (adapted from Koppitz et al. [31]); (b) steel straps anchored by bonding (adapted from Faria et al. [29])

Generally, effects of prestressing systems are three [32]:

- in-plane compression forces;

- deviation forces due to tendon inclination;
- bending moments due to tendon eccentricities;

In-plane forces affect both the load-rotation curve and the failure criterion curve. The compression field provides a greater flexural strength (V_R) and a stiffer behavior of the slab (Figure 22). Furthermore, in-plane compression forces enhance the interlocking strength provided by the critical shear crack [44]. Following Clement et al. [32] the failure criterion curve of a slab subjected to prestressing could be modified taking into account a reduced rotation (ψ'):

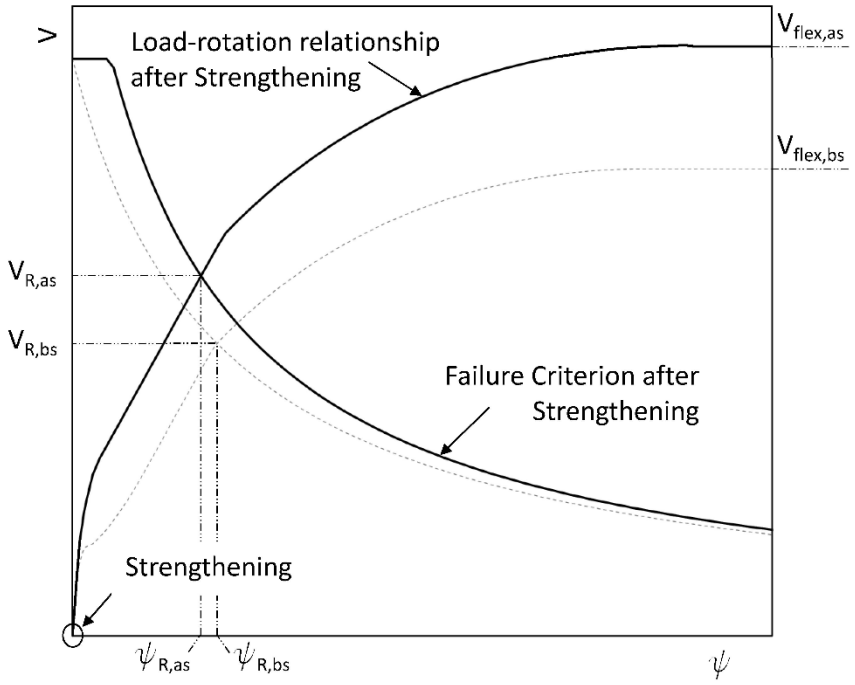

Figure 22 – Effects due to prestressing: in-plane forces

$$V_{c,pt} = \frac{3}{4} \cdot \frac{b_0 \cdot d \cdot \sqrt{f_c}}{1 + 15 \cdot \frac{\psi' \cdot d}{d_{g0} + d_g}} = \frac{3}{4} \cdot \frac{b_0 \cdot d \cdot \sqrt{f_c}}{1 + 15 \cdot \left(\psi + 45 \cdot \frac{\sigma_p}{E_c}\right) \cdot \frac{d}{d_{g0} + d_g}} \tag{23}$$

where σ_p is negative for compression stresses.

Deviation forces are represented by the vertical component of prestress forces resulting from inclined tendons near the column [45]. These forces are calculated at the intersection between the tendon and the critical surface (Figure 23). The latter, according to the CSCT, is placed at d/2 from the support. Therefore, the vertical component provided by the single tendon is equal to:

$$V_{P,i} = 2 \cdot \sin\beta \cdot P_i \tag{24}$$

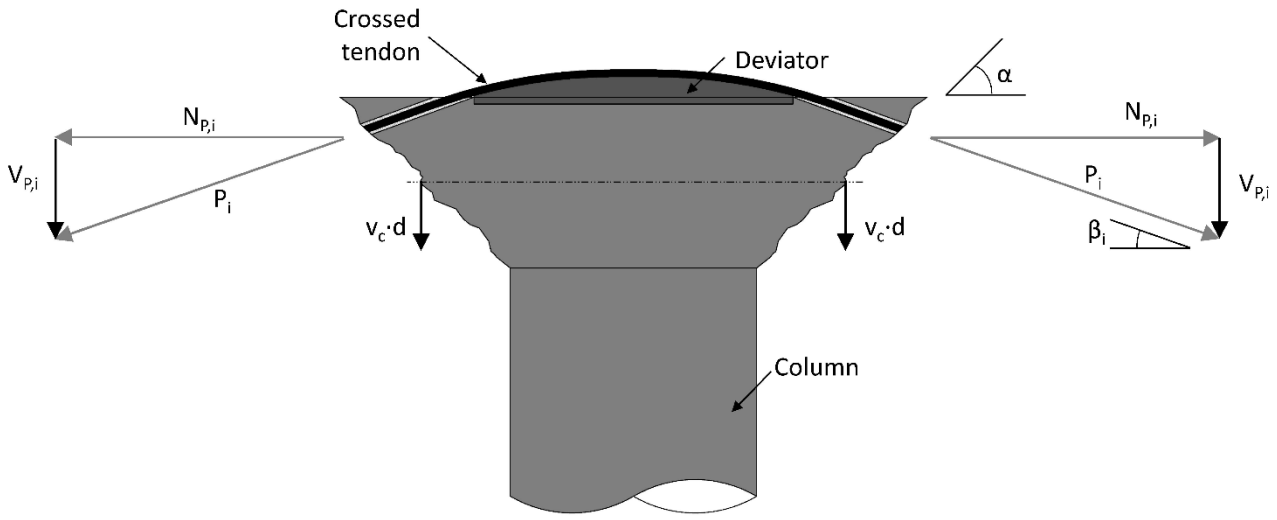

Figure 23 – Effects due to prestressing: reduction of shear force due to inclined tendons (adapted from Clement et al. [38])

where β is the inclination angle of the tendon and P is the prestress force. Deviation forces could be accounted for reducing external loads [46], [47] or increasing the punching strength [48]. Following the first approach the effective shear force becomes:

$$V_{eff} = V - V_P = V - \sum_{i=1}^{n} V_{P,i} = V - 2 \cdot \sum_{i=1}^{n} P_i \cdot \sin\beta_i \tag{25}$$

where the sum is extended to *n* tendons. However, in analogy with post-installed shear reinforcement, the second approach seems more suitable. Shear post-tensioning systems could be considered as particular cases of post-installed shear reinforcement, so the punching strength could be calculated according to equation (2):

$$V_{R,pt} = V_{c,pt} + V_P \tag{26}$$

where the contribution of the deviation forces (V_P) is accounted at varying the crack width (w_b) (see equations (5), (7) and (24)):

$$V_P = 2 \cdot \sum_{i=1}^{n} \left(P_i + E_s \cdot \frac{w_b}{l_s/2} \cdot A_s \right) \cdot \sin\beta_i \leq 2 \cdot \sum_{i=1}^{n} \left(A_s \cdot f_{ys} \right) \cdot \sin\beta_i \tag{27}$$

where A_s and l_s are the area and the length of the tendons, respectively. The half-length of the tendons instead of the whole length is accounted for the symmetry of the force system.

Finally, prestressing systems provide bending moments due to tendon eccentricities. These moments have opposite signs to those provided by external loads, thus they contribute to increase the punching strength. Following Clement et al. [32] the effect of these moments is calculated imposing the equilibrium of a sector of slab (Figure 24):

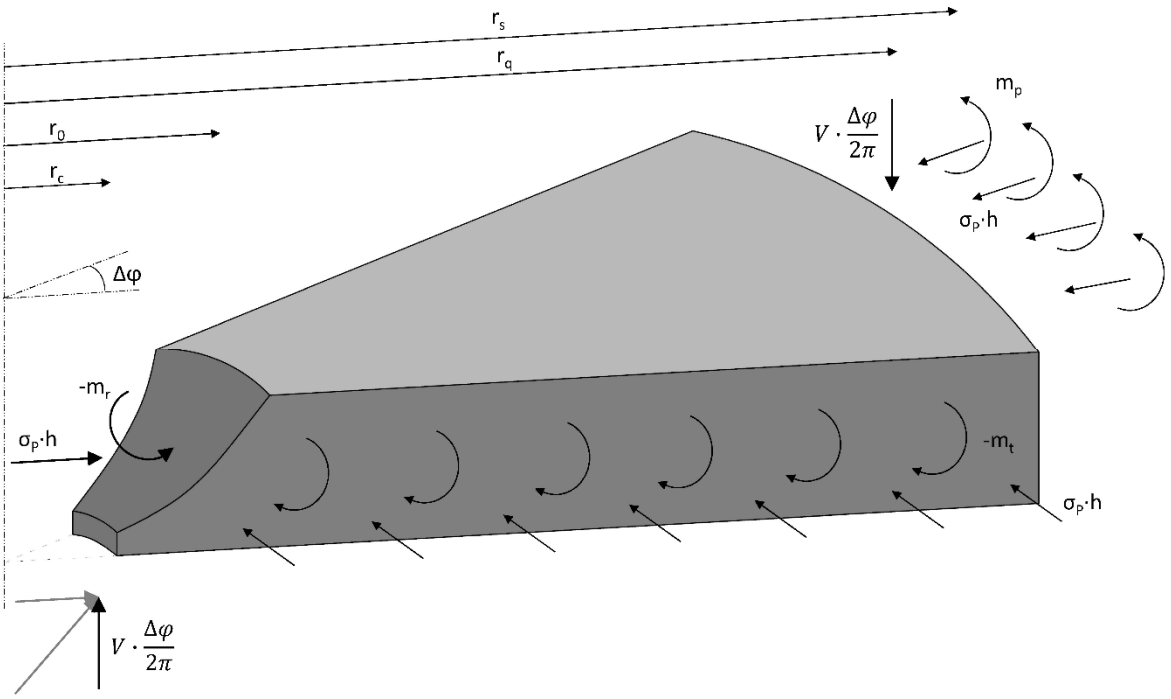

Figure 24 – Slab sector: equilibrium condition (adapted from Clement et al. [32])

$$V \cdot \frac{\Delta\varphi}{2\pi} \cdot (r_s - r_c) = -m_r \cdot \Delta\varphi \cdot r_0 + m_p \cdot \Delta\varphi \cdot r_m - \Delta\varphi \cdot \int_{r_0}^{r_s} m_t \cdot d_r \tag{28}$$

where r_m is the radius defining the area where the strengthening was performed. Therefore, the contribution provided by bending moments could be considered by raising the load-rotation curve (Figure 25) of the following amount:

$$V_{mp} = \frac{2\pi \cdot m_p \cdot r_m}{(r_s - r_c)} \tag{29}$$

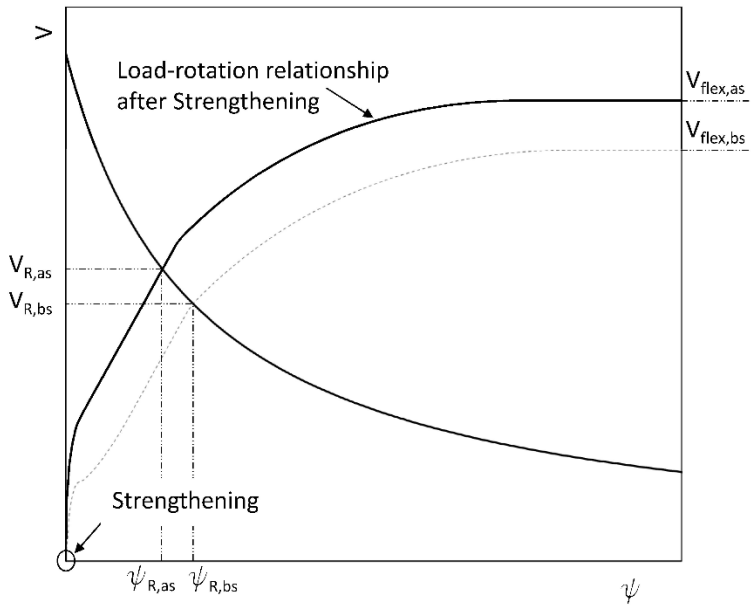

Figure 25 – Effects due to prestressing: bending moments due to tendon eccentricities

Flexural prestressing systems, as depicted in Figure 20, usually induce both in-plane compression forces and bending moments due to tendon eccentricities. However, experimental evidences about this technique are limited and results are not really convincing. Indeed, as shown by some authors [21], [22], in several cases limited improvements against punching are achieved since the occurrence of premature failure by debonding of anchorages.

On the contrary, as shown by several authors [28]–[31], shear prestressing systems (Figure 21) are more reliable and allow for considerable increase in punching capacity. Furthermore, the effectiveness of this technique is not affected by the initial slab rotation, shear post-tensioning rather allows for the slab deflection and crack width at service loads to be reduced [29]. For sake of simplicity the beneficial effect provided by tendon eccentricity could be neglected; following this approach the punching strength is provided by Equation (25). Finally, the presence of high deviation forces could bring to the crushing of the concrete strut [30]. For this reason, especially when V_P is greater than 50-60% V_c, the check against the concrete crushing is highly recommended. The latter is performed considering the entire shear force without any reduction due to the deviation forces. In Table 7 a comparison with experimental results is presented;

Table 7 – Main properties of literature experimental results and comparison with CSCT; $V_{th}=\min(V_{R,pt}; V_{flex}; V_{crush})$

Ref.	Spec.	Type[1]	d (mm)	ρ (%)	f_c (MPa)	P_0 (kN)	α (%)	V_{P0} (kN)	V_c (kN)	$V_{R,pt}$ (kN)	V_{crush} (kN)	V_{flex} (kN)	V_{exp} (kN)	V_{th} (kN)	V_{exp}/V_{th}
Faria et al. [29]	DF2	B	67	2.0	26.4	63	23	50	160	206	380	313	273	206	1.32
	DF3	B	67	2.0	25.2	59	22	46	157	200	364	309	255	200	1.27
	DF5	B	85	1.2	20.8	75	27	59	185	248	389	387	295	248	1.19
	DF6	B	84	1.3	21.0	70	26	55	186	233	388	383	293	233	1.26
	DF7	B	89	1.2	21.6	71	26	112	201	292	422	415	320	292	1.09
Keller et al. [30]	So1	A	194	1.6	39.9	317	47	1268	963	1947	1952	1975	1939	1947	1.00
	So2	A	199	1.6	40.7	217	49	868	1020	1660	2034	2036	1779	1660	1.07
	So3	A	204	1.5	40.3	225	66	900	1040	1691	2069	2091	1778	1691	1.05
	So4	A	199	1.6	40.9	102	15	408	1019	1359	2042	2037	1771	1359	1.30
														Avg	1.172
														CoV	0.097

P_0 is the initial prestress force applied in each tendon, P_u is the ultimate tensile strength of the tendon and $\alpha=P_0/P_u$. As shown before, shear prestressing systems are a very effective strengthening technique against punching. However, the maximum punching capacity is limited by the flexural strength and by the crushing of concrete strut. The latter could be calculated according to the Eurocode 2 (EC2-2004) [46].

4. DISCUSSION

In previous sections, the CSCT was applied to evaluate the punching capacity of R/C slabs strengthened using different strengthening techniques; in all cases, the theoretical results agree well with the experimental data. Table 8 lists the average value and the coefficient of variation of the ratio between the experimental and the theoretical punching capacity for each investigated strengthening technique. The average value ranges between 1.005 and 1.172, while the COV ranges between 0.026 and 0.097. The CSCT seems to provide the best results in terms of prediction capability for slabs strengthened using the BRCO or the enlargement of the support; nevertheless, further tests are required to validate these results, as available tests on slabs strengthened with one of these two techniques are very few. Conversely, many

experimental data are available for slabs strengthened with post-tensioning systems or post-installed shear reinforcement, so they are sufficient to validate the application of the CSCT to these techniques.

Table 8 – Applications of the CSCT to strengthened slabs, comparison with experimental results

Type	Number of specimens	Avg (V_{exp}/ V_{th})	CoV (V_{exp}/ V_{th})
Post-installed shear strengthening	37	1.036	0.078
Flexural strengthening (BRCO)	2	1.005	0.035
Enlargement of the support	5	1.024	0.026
Post-tensioning systems	9	1.172	0.097
	53	1.057	0.092

The application of the CSCT allowed main parameters affecting the punching capacity of strengthened slabs to be recognized for each strengthening technique. Moreover, thanks to the CSCT, the authors estimated the maximum capacity increment (ΔR) that each technique can provide and identified strong and weak points of each of them.

According to CSCT theoretical results, the use of post-installed shear reinforcement seems to be a very efficient and reliable strengthening technique. For the most specimens, the authors succeeded in designing the amount and type of shear reinforcement to avoid the punching failure, allowing for the ultimate flexural capacity of the slab to be reached. Only for a few specimens it was not possible to design the shear reinforcement to avoid the punching failure, because of the premature crushing of the concrete strut. Nevertheless, attention should be devoted to the activation phase of the shear reinforcement, as the effectiveness of the strengthening technique could be drastically reduced if the activation phase is too long. As the most effective method to shorten this phase is to prestress the reinforcement, bolts and studs anchored at both ends are preferred. Finally, the use of high strength materials for shear reinforcement is not required because the activation phase is governed by the slab rotation and the elastic modulus of reinforcement.

Flexural strengthening with FRP strips indirectly enhances the punching strength, as it increases the slab's stiffness. For this reason, the efficacy of this technique is strictly related to the amount of longitudinal reinforcement ρ of the existing slab; it decreases as ρ increases (for ρ<0.75% ΔR>20%, for ρ>1.00% ΔR<15%). The effectiveness is even lower when the strengthening is performed on loaded slabs (assuming V_{st}=50%·V_R, for ρ<0.75% ΔR>11%, for ρ>1.00% ΔR<6%).

The application of a BRCO provides better results when compared to FRP strips. Indeed, the increase of the slab's depth enhances the failure criterion, allowing for a greater punching strength to be reached (considering V_{st}=50%·V_R, for ρ<0.75% ΔR>60%, for ρ>1.00% ΔR<30%). Nevertheless, to avoid premature debonding of the R/C overlay, the use of mechanical connectors is recommended.

The enlargement of the support affects both the failure criterion and the load rotation relationship. However, the modification of the load-rotation curve is localized near the flexural plateau, so the initial slab rotation at the strengthening time does not affect the effectiveness of this technique. Furthermore, unlike other techniques, its efficacy is almost independent from the amount of longitudinal reinforcement of the existing slab. The main variable that affects the punching strength after strengthening is the ratio between the critical perimeter after and before strengthening ($b_{0,st}$/b_0). Assuming that the size B' of the enlarged

support is two times the existing column size (B'=2·B), the increase in punching strength is in the range 30÷50%.

Finally, shear post-tensioning systems could be treated as a case of post-installed shear reinforcement, where the punching strength after strengthening is given by two contributions: the concrete strength and the shear reinforcement strength. A proper design of the prestressing system can allow for the punching failure to be avoided and the ultimate flexural capacity to be reached in the strengthened slab. However, since the high deviation forces, a premature punching failure could occur due to the crushing of the concrete strut.

5. CONCLUSIONS

In this paper the main strengthening techniques against punching-shear were presented and discussed. Shear strengthening, flexural strengthening, enlargement of the support and post-tensioning systems are available techniques to improve the punching and flexural capacities of existing reinforced concrete flat-slabs. The authors applied the Critical Shear Cracks Theory (CSCT) to each strengthening technique to evaluate its efficacy against punching failure. The punching failure predictions provided by the CSCT, when compared with experimental results, show a good agreement. Considering more than fifty experimental results the average of the ratio between experimental and theoretical punching strength is $Avg(V_{exp}/V_{th}) = 1.06$ and the coefficient of variation is $CoV(V_{exp}/V_{th}) = 0.09$. In the light of these results, several parametric analyses were performed using the CSCT, which allowed for strong and weak points of each strengthening technique to be identified. Main results are summered in the following.

The use of post-installed shear reinforcement increases the punching strength as it raises the failure criterion; moreover, it also enhances the ductility. The efficacy of the strengthening is lower when performed on loaded slabs; nevertheless, this problem can be overcome using headed bolts and applying pre-stress in shear reinforcement.

Flexural strengthening is performed by gluing FRP or casting BRCO on the top of slabs. The first affects only the load-rotation curve, while the latter affects both the failure criterion and the load-rotation curve. The application of FRP is effective for low amounts of flexural reinforcement, while for high reinforcement ratios the increase of the punching strength is limited. The increase becomes even lower when the strengthening is performed on loaded slabs. The BRCO gives better results than gluing FRP strips, as it allows for the punching capacity to be increased by more than 20% also on loaded slabs and for high reinforcement ratios.

The enlargement of the support could be performed casting a new concrete capital or installing a steel capital. This strengthening technique affects both the failure criterion and the load-rotation curve, but its efficacy is not affected by the shear load at strengthening time. Considering a new support size equal to two times the existing support size, the punching strength increases by 30÷50%. Unlike other strengthening techniques, the efficacy of this technique is almost independent from the amount of flexural reinforcement of the existing slab.

Flexural and shear post-tensioning systems are also available for strengthening against punching-shear. However, flexural post-tensioning system showed several problems due to the failure of anchorages. On the contrary, shear prestressing systems are more reliable and allow for considerable increases in punching

capacity to be reached. The effectiveness of this technique is not affected by the time of strengthening, the results achieved on un-loaded or loaded slabs are expected to be almost the same. Furthermore, shear post-tensioning allows for reducing the slab deflection and crack width at service loads.

Finally, a combination of previous techniques could be used. For example, the use of FRP strips on the slab's top could be combined with post-installed shear strengthening. Doing so both flexural and shear strengthening are achieved. Either shear post-tensioning systems could be performed before the application of flexural strengthening like FRP or BRCO, to reduce the initial slab rotation and increasing the efficacy of the strengthening.

6. NOTATION

a_s longitudinal reinforcement cross-sectional area per unit length

$a_{s,st}$ longitudinal reinforcement cross-sectional area per unit length of the strengthening

A_{sw} cross-sectional area of a shear reinforcement

B support size

B' enlarged support size

b_0 perimeter of the critical section set at d/2 from the column

$b_{0,col}$ perimeter of the column

$b_{0,out}$ perimeter of the critical section outside the shear-reinforced zone

$b_{0,st}$ perimeter of the critical section of the strengthened slab

d effective depth

d_b diameter of shear-reinforcing bar

d_g maximum diameter of the aggregate

d_{g0} reference aggregate size (16 mm (0.63 in))

d_{inf} diameter of anchoring plate

d_{st} effective depth of the strengthened slab

d_v reduced effective depth

E_s modulus of elasticity of reinforcement

f_c average compressive strength of concrete

$f_{u,st}$ ultimate strength of the strengthening

f_y yield strength of flexural reinforcement

f_{yw} yield strength of shear reinforcement

h slab thickness

h_{BRCO} BRCO thickness

h_i vertical distance between the tip of the crack and the point where the shear reinforcement crosses the critical shear crack

L span of a slab

$l_{b,ii}$ distance between the point where a shear reinforcement is crossed by the critical shear crack and the lower end of the shear reinforcement (or the steel plate for anchored shear reinforcement)

l_{bsi} distance between the point where a shear reinforcement is crossed by the critical shear crack and the upper end of the shear reinforcement (or the steel plate for anchored shear reinforcement)

l_s the length of the post-installed bars or tendons

m_r ultimate bending moment of the slab section

n_a number of shear reinforcement per radius

n_r number of radii of shear reinforcement

P_i tensile force of the tendon after post-tensioning

P_u ultimate tensile strength of the tendon

r_c column radius

r_s distance between the column of a slab and the line of contraflexure of moments

s_r distance between two consecutive radii of shear reinforcement

V punching shear force

$V_{c,pt}$ concrete contribution to punching shear strength of slab strengthened with post-tensioning

V_{exp} measured punching shear load

V_{flex} shear force associated with flexural capacity of the slab

V_P deviation forces due to post-tensioning

V_R punching shear strength

$V_{R,as}$ punching shear strength after strengthening

$V_{R,brco}$ punching shear strength of slab strengthened with BRCO

$V_{R,bs}$ punching shear strength before strengthening

$V_{R,c}$ concrete contribution to punching shear strength

$V_{R,crush}$ punching shear strength, governing failure crushing of concrete strut

$V_{R,enl}$ punching shear strength of slab strengthened by enlargement of the support

$V_{R,in}$ punching shear strength, governing failure inside shear reinforced zone

$V_{R,out}$ punching shear strength, governing failure outside the shear reinforced zone

$V_{R,pt}$ punching shear strength of slab strengthened with post-tensioning

$V_{R,s}$ shear reinforcement contribution to punching shear strength

$V_{R,sr}$ punching shear strength with post-installed shear reinforcement

V_{serv} punching shear force at service load

V_{st} punching shear force at strengthening time

V_{th} theoretical punching shear prediction

w_b relative displacement of the lips of the critical shear crack parallel to shear reinforcement

α angle between the critical shear crack and the soffit of the slab

β angle between the shear reinforcement and the soffit of the slab

ρ flexural reinforcement ratio

ρ_w shear reinforcement ratio

σ_p negative compressive stress due to in-plan compression forces

σ_s steel stress

$\sigma_{s,b}$ maximum shear reinforcement stress due to bond failure

$\sigma_{s,el}$ steel stress during elastic activation of shear reinforcement

$\sigma_{s,p}$ maximum shear reinforcement stress due to pull-out failure

τ_b bond strength

ψ slab rotation

ψ' reduced slab rotation due to in-plane compression forces

ψ_{exp} measured rotation at failure

ψ_R slab rotation at failure

$\psi_{R,as}$ slab rotation at failure after strengthening

$\psi_{R,bs}$ slab rotation at failure before strengthening

ψ_{st} slab rotation at strengthening time

7. REFERENCE

[1] R. Koppitz, A. Kenel, and T. Keller, “Punching shear of RC flat slabs – Review of analytical models for new and strengthening of existing slabs,” *Eng. Struct.*, vol. 52, pp. 123–130, 2013.

[2] J. G. M. Wood, “Pipers Row Car Park , Wolverhampton Quantitative Study of the Causes of the Partial Collapse on 20 th March 1997,” 2003.

[3] N. J. Gardner, J. Huh, and L. Chung, “Lessons from the Sampoong department store collapse,” *Cem. Concr. Compos.*, vol. 24, no. 6, pp. 523–529, 2002.

[4] A. Ghali, M. A. Sargious, and A. Huizer, “Vertical Prestressing Of Flat Plates Around Columns,” *ACI Spec. Publ.*, vol. 42, pp. 905–920, 1974.

[5] G. Hassanzadeh, “Strengthening of bridge slabs with respect to punching. Test results. Report 41,” Stockholm, 1996.

[6] A. P. Ramos, V. J. G. Lucio, and P. E. Regan, “Repair and Strengthening Methods of Flat Slabs for Punching,” in *International workshop on punching shear capacity of RC flat slabs*, 2000, pp. 125–133.

[7] E. F. El-salakawy, M. A. Polak, and K. A. Soudki, “New Shear Strengthening Technique for Concrete Slab-Column Connections,” *ACI structral J.*, vol. 100, no. 3, pp. 297–304, 2003.

[8] M. M. G. Inácio, A. P. Ramos, and D. M. V Faria, “Strengthening of flat slabs with transverse reinforcement by introduction of steel bolts using different anchorage approaches,” *Eng. Struct.*, vol. 44, pp. 63–77, 2012.

[9] H. S. Askar, “Repair of R/C flat plates failing in punching by vertical studs,” *Alexandria Eng. J.*, vol. 54, pp. 541–550, 2015.

[10] H. S. Askar, “Usage of prestressed vertical bolts for retrofitting flat slabs damaged due to punching shear,” *Alexandria Eng. J.*, vol. 54, pp. 509–518, 2015.

[11] B. Binici, O. Bayrak, and M. Asce, “Punching Shear Strengthening of Reinforced Concrete Flat Plates Using Carbon Fiber Reinforced Polymers,” *J. Struct. Eng. ASCE*, vol. 129, no. 9, pp. 1173–1182, 2003.

[12] B. Binici and O. Bayrak, “Use of Fiber-Reinforced Polymers in Slab-Column Connection Upgrades,” *ACI structral J.*, vol. 102, no. 1, pp. 903–912, 2005.

[13] M. H. Meisami, D. Mostofinejad, and H. Nakamura, “Punching shear strengthening of two-way flat slabs using CFRP rods,” *Compos. Struct.*, vol. 99, pp. 112–122, 2013.

[14] M. H. Meisami, D. Mostofinejad, and H. Nakamura, “Punching Shear Strengthening of Two-Way Flat Slabs with CFRP Grids,” *J. Compos. Constr. ASCE*, vol. 18, no. 2, pp. 1–10, 2014.

[15] M. H. Meisami, D. Mostofinejad, and H. Nakamura, “Strengthening of flat slabs with FRP fan for punching shear,” *Compos. Struct.*, vol. 119, pp. 305–314, 2015.

[16] N. D. Gouveia, M. Lapi, M. Orlando, D. M. V Faria, and A. M. P. Ramos, “Experimental and theoretical evaluation of punching strength of steel fiber reinforced concrete slabs,” *Struct. Concr.*, vol. 19, no. 1, pp. 217–229, 2018.

[17] P. Schießl, *Zur Frage der zulässigen Rissbreite und der erforderlichen Betondeckung im Stahlbetonbau unter besonderer Berücksichtigung der Karbonatisierung des Betons*, no. 255. 1976.

[18] A. S. Mosallam and K. M. Mosalam, “Strengthening of two-way concrete slabs with FRP composite laminates,” *Constr. Build. Mater.*, vol. 17, pp. 43–54, 2003.

[19] U. Ebead and H. Marzouk, “Fiber-Reinforced Polymer Strengthening of Two-Way Slabs,” *ACI structral J.*, vol. 101, no. 5, pp. 650–659, 2004.

[20] C. Chen and C. Li, “Punching Shear Strength of Reinforced Concrete Slabs Strengthened with Glass Fiber-Reinforced Polymer Laminates,” *ACI Struct. J.*, vol. 102, no. 4, pp. 535–542, 2005.

[21] Y. J. Kim, J. M. Longworth, R. G. Wight, and M. F. Green, “Flexure of Two-Way Slabs Strengthened with Prestressed or Nonprestressed CFRP Sheets,” *J. Compos. Constr. ASCE*, vol. 12, no. 4, pp. 366–374, 2008.

[22] A. Abdullah, C. G. Bailey, and Z. J. Wu, “Tests investigating the punching shear of a column-slab connection strengthened with non-prestressed or prestressed FRP plates,” *Constr. Build. Mater.*, vol. 48, pp. 1134–1144, 2013.

[23] M. R. Esfahani, M. R. Kianoush, and A. R. Moradi, “Punching shear strength of interior slab – column connections strengthened with carbon fiber reinforced polymer sheets,” *Eng. Struct.*, vol. 31, pp. 1535–1542, 2009.

[24] D. M. V Faria, J. Einpaul, A. P. Ramos, M. Fernández Ruiz, and A. Muttoni, “On the efficiency of flat slabs strengthening against punching using externally bonded fibre reinforced polymers,” *Constr. Build. Mater.*, vol. 73, pp. 366–377, 2014.

[25] A. Muttoni, “Punching shear strength of reinforced concrete slabs without transverse reinforcement,” *ACI Struct. J.*, vol. 105, no. 4, pp. 440–450, 2008.

[26] G. Hassanzadeh and H. Sundqvist, “Strengthening of bridge slabs on columns,” *Nord. Concr. Res.*, vol. 21, pp. 23–34, 1998.

[27] Widianto, “Rehabilitation of Reinforced Concrete Slab-column Connections for Two-way Shear,” University of Texas at Austin, 2006.

[28] D. M. V Faria, V. J. G. Lucio, and A. P. Ramos, “Strengthening of reinforced concrete slabs using post-tensioning with anchorages by bonding,” in *Proceedings of the Annual International fib Symposium Concrete : 21st Century Superhero*, 2009.

[29] D. M. V Faria, V. J. G. Lúcio, and A. P. Ramos, “Strengthening of flat slabs with post-tensioning using anchorages by bonding,” *Eng. Struct.*, vol. 33, pp. 2025–2043, 2011.

[30] T. Keller, A. Kenel, and R. Koppitz, “Carbon Fiber-Reinforced Polymer Punching Reinforcement and Strengthening of Concrete Flat Slabs,” *ACI Struct. J.*, vol. 110, no. 6, pp. 919–928, 2013.

[31] R. Koppitz, A. Kenel, and T. Keller, “Punching shear strengthening of flat slabs using prestressed carbon fiber-reinforced polymer straps,” *Eng. Struct.*, vol. 76, pp. 283–294, 2014.

[32] T. Clément, A. P. Ramos, M. Fernández Ruiz, and A. Muttoni, “Influence of prestressing on the punching strength of post-tensioned slabs,” *Eng. Struct.*, vol. 72, pp. 56–69, 2014.

[33] J. Longworth, L. Bizindavyi, R. G. Wight, and A. Erki, “Prestressed CFRP sheets for strengthening two-way slabs in flexure,” in *Proc., 4th Int. Conf. on Advanced Composite Materials in Bridges and Structures (ACMBS-IV)*, 2004.

[34] H. Fernandes, V. Lúcio, and A. Ramos, “Strengthening of concrete flat slabs with an overlaid reinforced concrete layer,” in *fib Symposium 2016 - Performance-based Approaches for Concrete Structures*, 2016.

[35] H. Fernandes, V. Lúcio, and A. Ramos, “Strengthening of RC slabs with reinforced concrete overlay on the tensile face Adhesion / Interlocking + Friction,” *Eng. Struct.*, vol. 132, pp. 540–550, 2017.

[36] M. Lapi, H. Fernandes, M. Orlando, A. P. Ramos, and V. J. G. Lucio, “Performance assessment of flat slabs strengthened with a bonded reinforced concrete overlay,” *Mag. Concr. Res.*, 2017.

[37] M. F. Ruiz, A. Muttoni, and J. Kunz, “Strengthening of flat slabs against punching shear using post-installed shear reinforcement,” *ACI Struct. J.*, vol. 107, no. 4, pp. 434–442, 2010.

[38] T. Clément, A. P. Ramos, M. F. Ruiz, and A. Muttoni, “Design for punching of prestressed concrete slabs,” *Struct. Concr.*, vol. 14, no. 2, pp. 157–167, 2013.

[39] R. Koppitz, A. Kenel, and T. Keller, “Effect of load history on punching shear resistance of flat slabs,” *Eng. Struct.*, vol. 90, pp. 130–142, 2015.

[40] R. Koppitz, “Effect of Deformation History on Punching Resistance of Reinforced Concrete Slabs PAR,” vol. 6472, 2015.

[41] M. F. Ruiz and A. Muttoni, “Applications of critical shear crack theory to punching of reinforced concrete slabs with transverse reinforcement,” *ACI Struct. J.*, vol. 106, no. 4, pp. 485–494, 2009.

[42] R. V. Rodrigues, M. F. Ruiz, and A. Muttoni, “Paper published by the Structural Concrete Laboratory of EPFL Title : Authors : Published in : Volume : Pages : Country : Year of publication : Punching shear strength of R / C bridge cantilever slabs Vaz Rodrigues R ., Fernández Ruiz M ., Muttoni A . Typ,” vol. 30, no. 3, pp. 3024–3033, 2008.

[43] M. H. Sharaf, K. A. Soudki, and M. Van Dusen, “CFRP Strengthening for Punching Shear of Interior Slab – Column Connections,” *J. Compos. Constr. ASCE*, vol. 10, no. 5, pp. 410–418, 2007.

[44] A. P. Ramos, V. J. G. Lúcio, and P. E. Regan, “Punching of flat slabs with in-plane forces,” *Eng. Struct.*, vol. 33, pp. 894–902, 2011.

[45] A. P. Ramos, V. J. G. Lúcio, and D. M. V Faria, “The effect of the vertical component of prestress forces on the punching strength of flat slabs,” *Eng. Struct.*, vol. 76, pp. 90–98, 2014.

[46] CEN, *Eurocode 2: Design of concrete structures - Part 1-1: General rules and rules for buildings*. Bruxelles, 2004.

[47] CEB/FIP, *Model Code 2010 - Volume 1*, Bulletin 6. Lausanne, switzerland: Internation Federation for Structural Concrete (fib), 2012.

[48] ACI Committee 318, *Building Code Requirements for Structural Concrete (ACI 318M-14) and Commentary (ACI 318RM-14)*. Farmington Hills, U.S.A., 2014.